Universitat Autònoma
de Barcelona

A thesis for the

Master in Telecommunications Engineering

MIMO demonstrator using FMCOMMS5-EBZ evaluation board

Miquel Perelló Serrano
miquel.perellos@e-campus.uab.cat

Supervisor: Josep Parrón Granados
Josep.Parron@uab.cat
Department of Telecommunications and Systems Engineering
Universitat Autònoma de Barcelona (UAB)
Escola d'Enginyeria

February, 2022

RESUM:

El món està evolucionant, i la globalització ha permès que tothom estigui connectat a tot el que ens envolta i puguem comunicar-nos a grans distancies. Això causa que els dispositius de comunicació cada vegada necessitin més capacitat i velocitat de transmissió de dades. Per tal d'aconseguir-ho noves tecnologies estan sorgint, i una d'elles és la transmissió MIMO. Aquesta transmissió ens permet dividir un canal de transmissió entre diverses antenes de transmissió i diverses antenes de recepció. Ampliant la capacitat del canal i permetent moltes més transmissions de les que podíem fer anteriorment.

En aquest projecte es presentarà la metodologia per dissenyar crear un array d'antenes per tal de poder crear aquesta transmissió. A la vegada de la comprovació de que aquesta divisió del canal es pugui realitzar i quines limitacions té.

RESUMEN

El mundo está evolucionando, y la globalización ha permitido que todos estén conectados a todo lo que nos rodea y podamos comunicarnos a grandes distancias. Esto causa que los dispositivos de comunicación cada vez necesiten mayor capacidad y velocidad de transmisión de datos. Con el fin de conseguirlo nuevas tecnologías están surgiendo, y una de ellas es la transmisión MIMO. Esta transmisión permite dividir un canal de transmisión entre varias antenas de transmisión y varias antenas de recepción. Ampliando la capacidad del canal y permitiendo muchas más transmisiones de las que podíamos realizar anteriormente.

En este proyecto se presentará la metodología para diseñar crear un array de antenas para poder crear esta transmisión. A la vez que la comprobación de que esta división del canal se pueda realizar y qué limitaciones tiene.

SUMMARY

The world is evolving, and globalization has allowed everyone to be connected to everything around us and to be able to communicate over long distances. This means that communication devices need more and more capacity and speed of data transmission. New technologies are emerging, and one of them is MIMO transmission. This transmission allows us to divide a transmission channel between several transmitting antennas and several receiving antennas. Expanding the capacity of the channel and allowing many more transmissions than we could do before.

This project will present the methodology for designing the creation of an antenna array in order to create this transmission. At the same time checking that this division of the channel can be done and what limitations it has.

Acknowledgements

I would like to thank professor Josep Parron for giving me the opportunity of working at this project, being available to all the questions I had during the project.

Thanking the other students working with me, giving ideas and making the environment so positive.

And finally thanking Ernesto for milling and weld all the designs I made.

Contents

List of Figures

List of Tables

Chapter 1

Introduction

Communication has become one of the priorities of our society. We want to know everything that happens around and at the other side of the globe. This causes the need to transmit increasingly more data to fullfil this lifestyle. That means, wireless data transmission is the most used communication nowadays. This transmission has the function to allow this all-communicated world, without the need of wires that would make a negative visual impact and a difficult management of the networks. It is logical that this field is being studied and improved constantly in order to increase communication capacity, transfer velocity and the reduction of its latency and many other features of communications. This constant evolution of communications to improve its features, has meant that governments of each country have been involved in the new applications, and which frequencies they must use[4]

Thanks to this new technologies being implemented, some others that were discovered but not used because of the lack of resources are now starting, such as MIMO [1]. The development of of wireless communication systems has raised the requirements of wireless communication systems. It has become increasingly difficult to fullfil these requirements with traditional SISO (single-input single-output) systems, due to the limitations in channel capacity [5]. However, by using multiple input (transmitters diversity) and multiple output (receivers diversity), MIMO systems are able to transmit multiple decorrelated signals, with the same power level, simultaneously through spatially parallel channels. One of the main benefits of MIMO systems over traditional SISO systems are their improved capacity and reliability, without increasing transmitted power or bandwidth. In a MIMO system, the antennas not only have a great impact on the system's received channel capacity, but they also play an important role in system stability. The design of antenna arrays optimised for different diversity schemes and the impact from the environment on the antenna arrays are important current research topics for MIMO systems.

The need of being able to communicate faster, safer and easier whenever and wherever, means that the devices needs a more complex technology at the front-end but also at the back-end (software) that runs it. To do so, new technologies have been implemented. This is the case of 5G technology, that thanks to new technologies in signal processing, hardware on high frequencies, will allow anything society wants. In order to do so, a new frequency allocation policy has been made by governments to obtain a good combination of coverage and capacity benefits. The 5G frequency selected range is the 1-6GHz that will include the 3.3-3.8 GHz range. This range is expected to be the foundation of many early 5G

services and applications [6].

1.1 State of the art

MIMO term comes from "Multiple-Input Multiple-Output", meaning that we are transmitting with several devices, and also receiving with multiple devices, but at the end all the data is treated as a single scenario. In our case, this will imply a several transmitting antennas and also multiple receiving antennas. It works using multi-channel transmission (the different paths the signal can travel until it arrives to the receiver).

The first time the MIMO concept was introduced, was in the middle 80's, by Jack Salz who was investigating multi-users systems [7]. However, it was not until 1994 when a patent using a SDMA-based inverse multiplexing technique in order to improve the performance of cellular radio network [8]. Later on 2004, the first product using MIMO technology was commercialised: The WiFi standard 802.11n [9].

Although it was discovered long time ago, in order to use MIMO with good efficiency, a cluster of separated antennas was needed in the same device. The fact that the frequencies used were low, caused that the antennas were too big[1] to implement an array of it in the same device, preventing MIMO applications on being used. Thanks to the new technologies implemented for high frequencies, new applications are being allocated at this "medium-high" frequencies that will make our device smaller. This is allowing the implementation of MIMO these days in our phones, laptops.

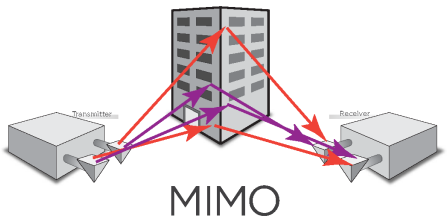

Figure 1.1: MIMO representation

The 5G technology is now being implemented in order to improve the latency and capacity of the transmissions. The role of MIMO in these applications will be allowing this amount of data to be transmitted and received by the devices. A few of the improvements of MIMO applications are the following:

- Beamforming + MIMO [10]: Combining it with the beamforming will add a better radiation diagram to our array. This will improve the efficiency of our device and at the same time will add the different channels MIMO technology needs to work properly.

[1] Remember that the antennas dimensions and its separation is directly related to the wavelength, that is the inverse of the frequency

- MU MIMO [11]: Multi-user MIMO, consists on distributing the great number of the transmitter antennas MIMO needs to work, between multiple connected users. This feature will reproduce the spacing between antennas needed for the MIMO application, and it will not be necessary to do it on every device. It is important to remark that all transmitting antenna must be fed at all time, since with just one, MIMO features are not possible.

- Software defined radio system (SDR) [12]: An SDR is a collection of hardware and software technologies that enable reconfigurable system architectures for wireless networks and user terminals. It provides an efficient and comparatively inexpensive solution to the problem of building multi-mode, multi-band, multi-functional wireless devices that can be enhanced using software upgrades. In our case the SDR module FMCOMMS5-EBZ evaluation board will allow us to develop the MIMO transmission in any frequencies within the range of 70MHz to 6GHz.

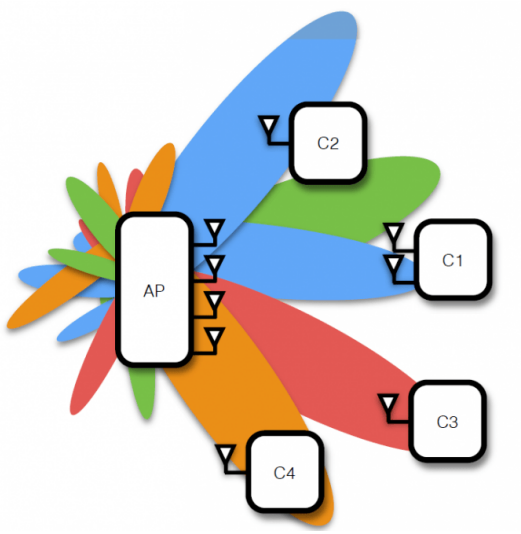

Figure 1.2: Multi-User MIMO representation [1]

1.2 Objectives

In this project we can distinguish two main objectives:

1. Design, fabricate and characterise an array of 4 patch antennas. The basic requirement of the array is that it must work at 3.6GHz, since as we have described earlier, this band will be used for many 5G services. Another requirement is that the dimensions must not surpass the 290x210mm, which is the maximum length our milling machine can operate with.

2. The second main objective is the implementation of a MIMO transmission using SDR. Before that, of course, the main concepts behind MIMO will be explained in order to create a simulated transmission.

1.3 Project organisation

This project will be organised in two parts:

1. **Antenna fabrication**: Firstly we will clarify the concepts of the operation of the antennas in Chapter2. After this, the procedure to fabricate the antenna will start, that will be seen in Chapter3:

   - Design and simulation: Feko electromagnetic software [13] will be used in order to design our array of antennas, with the desired features such as the working frequency, bandwidth, coupling between patches and many others. Once all these features are considered correct the fabrication of the antenna will be made.
   - Measurement: In order to know that the antenna is working at the correct frequency and is well matched and isolated, a network analyser will be used. The results will be compared and analysed with the simulation results to find discrepancies and the their reason. Finally, the radiation diagram, the gain and efficiency will be measured in an anechoic chamber.

2. **MIMO application**: To apply the array on a MIMO application, an introduction of the basic concepts will be made in Chapter4. This will help to recreate and validate various simulated scenarios of a MIMO transmissions on Matlab [14].

   Once the simulation is done, we will recreate the scenario on the anechoic chamber with the array previously fabricated. Once this is finished a comparison between the measurements and the simulation will be made, in order to obtain the features of the design, such as the noise, SNR[2], BER[3] noise power, signal power and relative error. This measurements will help optimise the transmission code.

1.3.1 Software used

The different software used in the project are the following ones:

- FEKO [13]: Electromagnetic simulation software tool for the electromagnetic field analysis of 3D structures. It offers multiple state-of-the-art numerical methods for the solution of Maxwell's equations. This software allow us to recreate scenarios of the antennas to find the features wanted from it.
- MATLAB [14]: Programming and numeric computing platform, to analyse data, develop algorithms, and create models. This software will be used in order to simulate a MIMO transmission, and at the same time, connect to the SDR FMCOMMS5-EBZ evaluation board to the anechoic chamber so a real transmission can be made.

1.3.2 Devices used

The devices used in order to carry out the project are the following ones:

[2]Signal-to-noise ratio
[3]Bit error rate

- LPKF ProtoMat S62[15]: It is an advanced PCB prototyping with a precision of 0.25μm, and a maximum dimensions of an A4 (297x210mm) that will establish one of the features of the array. This milling machine will be used in order to fabricate the array of four antennas that will be simulated on FEKO.

Figure 1.3: LPKF ProtoMat S62

- FMCOMMS5-EBZ evaluation board[16]: The AD-FMCOMMS5-EBZ is a high-speed analog module designed to showcase the AD9361 in multiple-input, multiple-output (MIMO) applications. The AD9361 is a high performance, highly integrated RF transceiver that operates from 70 MHz to 6 GHz, and supports bandwidths from less than 200 kHz to 56 MHz. The AD-FMCOMMS5-EBZ supports dual AD9361 devices, allowing for the creation of a 4x4 MIMO system. Since this device supports a 4 input and a 4 output signal, the idea is to prove a 4x4 MIMO transmissions with the fabricated antenna array.

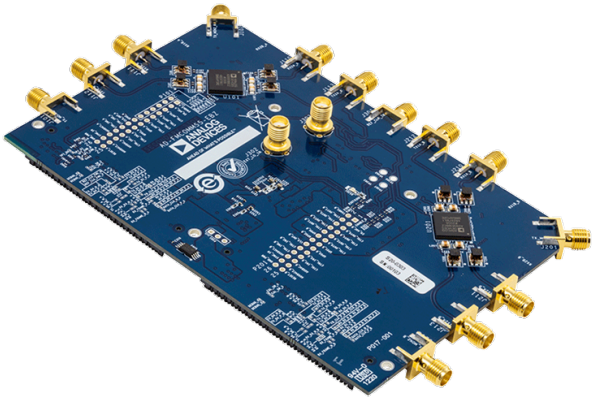

Figure 1.4: FMCOMMS5-EBZ evaluation board

- N5242A Network analyzer[17]: This network analyser is an integrated test system for complete linear and non-linear characterisation of RF and microwave components and devices with

a single set of connections. The analyser is a four-port, double-source instrument. This instrument will allow us to measure the matching of the fabricated array.

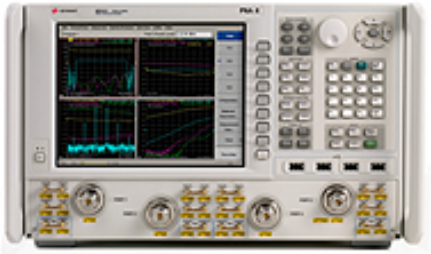

Figure 1.5: N5242A Network analyzer

- Anechoic Chamber: The anechoic chamber where this measurement will be made is situated in space QC-1035 of the Department of Telecommunication and Systems Engineering at the Autonomous University of Barcelona. It has a dimension of 5x3x3 meters, and its outer is made by a combination galvanised steel and wood preventing outer interference to enter the chamber (at least attenuated more than 60dB) . Adding the inner walls floors and ceiling with polyurethane foams pyramid-shaped carbon doped to absorb electromagnetic radiation and prevent the signal reflections. All of this allows the characterisation of antennas and RF devices.

  Some images of the anechoic chamber can be seen in Figure 1.6.

(a) Outside of the anechoic chamber (b) Inside the anechoic chamber

Figure 1.6: Anechoic chamber

The chamber has one static mast and another moved by an positioner controlled from the outside with a Controller ASYCONT and software ASYSOFT [**?**], that will allow us to move

one of the antennas (in our case the transmitter), in order to have a 3D radiatio pattern. This positioner provides a precision of 0.1° both in azimuth and elevation. The distance between the masts is 2.6 meters(31.2λ at 3.6GHz).

Chapter 2

Patch antenna theory

As most of the microelectronics technology on PCB, the idea of patch antennas was developed on the 50's, but was not until 1972 when they were fully applied. Since then, this type of antenna have been the most common type of antenna.

In this section, we will clarify all the basic concepts of patch antennas in order to understand what are we simulating and the different obtained results, the information is extracted from [18] and [19].

2.1 Fundamental parameters of antennas

An antenna is the part of the transmitting or receiving system that is designed to transmit o receive electromagnetic waves. An electromagnetic wave is a disturbance of the electric and magnetic fields which is propagated through space. This disturbance is characterised by its frequency f and its wavelength λ. The velocity the wave is propagating v_p,(normally considered the speed of light) must the the product between this variables (2.1):

$$v_p = f\lambda \tag{2.1}$$

2.1.1 Antenna as a circuital element

Firstly, it is important to characterise how well matched is the antenna to the system it is connected. An schema of the antenna and feeding source is seen in Figure2.1

The matching between the antenna and the transmitter/receiver can be described as a how much of the feeding source wave is reflected when entering the antenna, being a good matching a no reflection wave [20]. Numerically, it can be represented as the power wave reflection coefficient (2.2), that quantifies the level of the incident waveform that is reflected where Z_a is the antenna impedance and Z_o the source impedance. Ideally this the value of S to be 0, since it means that the propagation wave does not reflect when it enters the antenna. Another variable defining the antenna matching to the feeding source is the reflection efficiency (2.3)

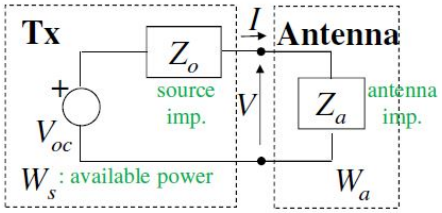

Figure 2.1: Antenna characterised as a circuital element

$$S = \frac{Z_a - Z_o^*}{Z_a + Z_o} \tag{2.2}$$

$$e_r = 1 - |S|^2 \tag{2.3}$$

The antenna input impedance Z_a seen in (2.4) can be divided into the antenna resistance R_a as the real part, and the antenna reactance X_a as the imaginary. The antenna resistance can be divided into radiated resistance R_r and loss resistance R_Ω:

$$Z_a = \frac{V}{I} = R_a + jX_a = (R_r + R_\Omega) + jX_a \tag{2.4}$$

The radiation efficiency e_{cd}(2.5), is defined as the ratio of the total power radiated by an antenna to the net power accepted by the antenna from the connected transmitter:

$$e_{cd} = \frac{R_r}{R_a} \tag{2.5}$$

By doing an analysis of the system link budget we can also extract some important information. Given the available power of our system W_s and the reflection efficiency (2.3), we can extract the power delivered to the antenna W_a (2.6). At the same time, knowing this delivered power and the radiated power of the antenna (2.7) given by the radiation resistance R_r, we determine the radiation efficiency of the antenna (2.8):

$$W_a = W_s \cdot e_r \tag{2.6}$$

$$W_r = |I|^2 R_r \tag{2.7}$$

$$e_{cd} = \frac{W_r}{W_a} \tag{2.8}$$

2.1.2 Antenna as a radiating element

The other key factor of the antenna, is how it is radiating the signal. Given the electric $\vec{E}$ and the magnetic field $\vec{H}$ with a time-harmonic variation, like most of the signals, we can establish the average power radiated by the antenna is transmitting per unit area (2.9). This average power is measured depending on the spherical coordinates Θ and ϕ

$$\vec{P}_{av}(\Theta,\phi) = \frac{\left|\vec{E}\right|^2}{\eta}\hat{r} = \eta\left|\vec{H}\right|^2\hat{r} \tag{2.9}$$

Where $\hat{r}$ is the unitary vector of the space, and $\eta = 120\pi\Omega$ is the vacuum characteristic impedance .

Integrating the average power density per unit area P_{av} in a sphere, the radiated power (2.7)[20].

In the power of the antenna, the polarization is a property applying to transverse waves that specifies the geometrical orientation of the oscillations. We could define 2 different polarization.

- Copolar: Component of the radiated field that is received by an application. Defines the power that we are able to receive and use.
- Crosspolar: Component of the radiated field that is orthogonal to the copolar component. Basically is power that is not able to be received by the application.

In order to have a graphical representation of the radiation properties of the antenna, the radiation pattern is the tool used. It gives information of the 2 2D cuts (E plane and H plane) of the coordinate axis.

This radiation pattern also gives the information of:

- Half power beamwidth(HPBW)[21]: Angle between the half power points of the main lobe as measured at -3dB
- First null beamwidth (FNBW): Degree of angular spacing from the main beam.
- Side lobe ratio(SLR): Ratio of the amplitude at the peak of the main lobe to the amplitude at the peak of a side lobe.
- Front to back ratio (FBR): Ratio of power radiated in the front/main radiation lobe and the power radiated in the opposite direction

Directivity is another important feature of the antennas, since it measures the degree to which the radiation emitted is concentrated in a single direction. For a directive antenna (it may not be the case), the maximum directivity corresponds to (2.10).

$$D_{max} = \frac{1}{\frac{1}{4\pi}\int_0^{2\pi}\int_{0)}^{\pi}|F(\Theta,\phi)|^2 sin\Theta d sin\Theta d\phi} \tag{2.10}$$

And finally the antenna gain G is the ability of the antenna or antenna system to direct the radiated power in a specific direction or conversely, absorb the power efficiently coming from a particular direction[22](2.11).

$$G = D_{max}e_{cd} \tag{2.11}$$

2.2 Theory of patch antennas

Along the years, electronics have been on a constant development, always finding new applications, with more components, more wires and better features. However, as it is logical to think, designing all the circuitry with all the components to give the service it is made for, started to be quite difficult. This difficulty is due to the fact that all the connections were start-end, and they were too big to fit on the other devices. So at the beginning of the 20th century some research begin to study how to compact the designs. Since then, the field has not stopped developing, firstly for military purpose and finally for all kind of applications to the public. One of the many applications, is a patch antenna, that thanks to its low profile and easy implementation, allows to receive and transmit signals from really small and portable devices.

Once the basic concepts and features of an antenna are described, we should be able to describe more accurately the functioning of a patch antenna.

A patch antenna is a type of antenna with a low profile, which can be mounted on a surface. It consists of a planar rectangular, circular, triangular, or any geometrical sheet or "patch" of metal, mounted over a larger sheet of metal called a ground plane. They are the original type of microstrip antenna described by Howell in 1972; the two metal sheets together form a resonant piece of microstrip transmission line with a length of approximately one-half wavelength of the radio waves[23]. The main parameters that will contribute to the patch radiation are in the following Figure 2.2.

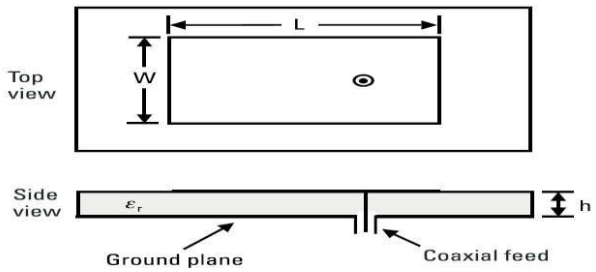

Figure 2.2: Microstrip patch antenna components

The basic equation to take into account when designing a patch antenna is which frequencies and which modes are being excited:

$$(f_r)_{mnp} = \frac{1}{2\pi\sqrt{\mu\epsilon}}\sqrt{(\frac{m\pi}{h})^2 + (\frac{n\pi}{L})^2 + (\frac{p\pi}{W})^2} \qquad m,n,p : 1,2,3.. \tag{2.12}$$

Where m,n,p determine a mode and can not be 0 simultaneously. The variables μ and ϵ are the Magnetic permeability and electrical permittivity in vacuum respectively. This is important since we will have to determine which is the mode we want to excite in order to make it the dominant and put it at the frequency we want. Usually the excited mode will s be the mode TM_{010} since it is the one that has a radiation pattern orthogonal to the antenna and its easier to use.

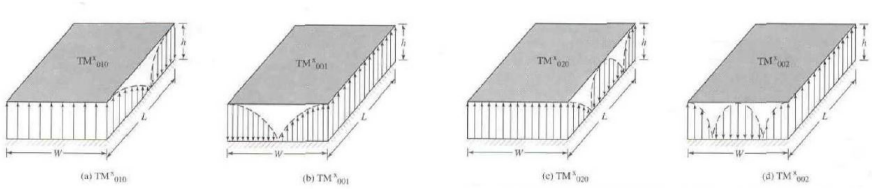

Figure 2.3: Mode excitation

The Figure2.3 shows how he electric field is distributed along the patch in different modes. This will be important in order to know where the feeding point needs to be, in order to excited the desired mode and which input impedance the antenna has.

Considering the dominant mode TM_{010}, and a rectangular shape the different metrics of figure have the following impact 2.2:

- L: Will be used in order to obtain the operating frequency, depending on its dimension
- W: Will be used to match the antenna and obtain a good radiation efficiency
- h: Will determine the high of the dielectric, it must be much lower than the wavelength. It will have a direct influence on the reactance the antenna has making easier or harder the matching of the antenna.
- e_r (dielectric constant): Depending on the material. It may vary from 2.2 to 12. If it is smaller, the size of the antenna will be larger but efficient. A large dielectric constant, will make our antenna smaller but less efficient.

Another important fact about the patch antenna is the feeding point. It will depend on which mode the antenna is being excited. For example, in mode TM_{010}, the feeding point must be in the centre of the W, since the nearest mode(TM_{001}) (in frequency) has no fields in that position. At the same time, changing the feeding point along the L dimension, will allow to obtain the input impedance wanted. Remember that when no fields are transmitting, the antenna can be seen as an open circuit where the input resistance (2.4) is ∞ and when the maximum fields are transmitted, the antenna can be seen as a short-circuit where the input impedance is null. In order to find the desired input impedance (in our case 50Ω since is the impedance of the output ports of the FMCOMMS5-EBZ evaluation board), we will have to obtain the spot along the L dimension where the impedance is 50Ω.

There are a few feeding techniques for a patch antenna that will be described below

- **Coaxial probe:** Consists on introduce a probe, that crosses the dielectric, don't touches the ground plane to avoid a short circuit, and feeds the patch as in Figure2.2. It 's really easy to implement, but at high frequencies, it can be difficult to find an input match for the antenna due to probe inductance.
- **Proximity coupling:** In this case, the geometry consists that between the ground and the patch, there will be the microstrip line.

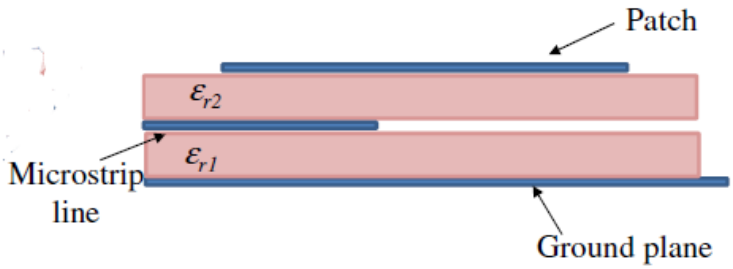

Figure 2.4: Proximity coupling feeding technique

- **Aperture coupled:** Same theory as the previous technique, but instead of the microstrip line between the patch and the ground, it is under the ground, and this one has an aperture that leads the radiation to the patch.

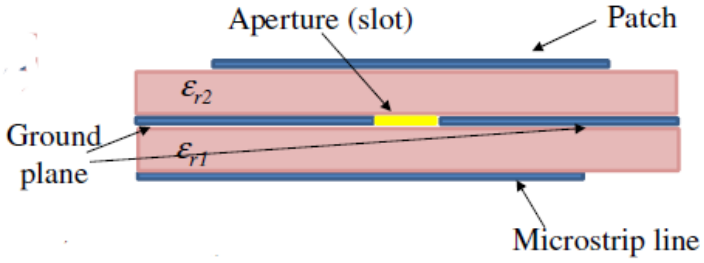

Figure 2.5: Aperture coupled feeding technique

- **Microstrip line:** The metallic patch of an antenna is fed via a lesser width of the microstrip line as compared to the patch in the same plane. So a single structure is made by the feeding and the patch.

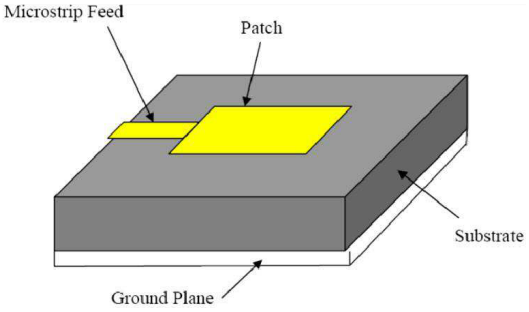

Figure 2.6: Microstrip line feeding technique

Chapter 3

Design and measurement of the antenna

In this chapter, the design and measurement of the four patch antenna array will be explained. The basic features is that the array must work at 3.6 GHz and it cannot surpass the 290x210mm, in order to be able to fabricate it in the milling machine and measure it with our equipment.

3.1 Design

Before starting with the full design of the four patch antenna array, which is the main goal, we considered important to match the antenna well at 3.6GHz just one patch in order to know which were the main characteristics that needed to be changed. Since FEKO is a software that computes the different parameters demanded upon the number of surface mesh triangles in which the area of the element is divided, and therefore, for how many areas the Maxwell equations will be computed. The basic procedure of the antenna's matching will be execute a low precise simulation with small amount of elements (that is one of the reasons we start matching just 1 patch antenna) with infinite substrate, and end with high accuracy simulations with a more real model in order to find the most realistic antenna features.

The restrictions of the antenna array are the following:

- Needs to work at 3.6GHz
- The array must not surpass the 290x70mm
- Matched to 50Ω since the board FMCOMMS5-EBZ output ports have this characteristic impedance.

At the same time since the easiest way to feed the antenna was with a via, because in the laboratory we already have the connectors. At the same time the milling machine has the precision to make it with a radius of 0.65mm that is more than enough precision for our project.

3.1.1 1 patch antenna design

Given that the the restrictions of the design doesn't tell anything about the efficiency nor the minimum value of the reflection coefficient at the desired frequency, could be interesting to find which material is allowing the best performance of the antenna. So meanwhile the matching of 1 patch is done, an analysis of different materials will be made.

To match the antenna at the desired frequency given a substrate were the height is given and the dielectric constant too, the only values that can be changed in order to match the antenna at a certain frequency are the length L and the width W.

The values of the width and the length can be determined, by choosing the dominant mode of the application, which in our case will be the the TM_{010}. Knowing this, and with the equation of resonant frequencies of a patch antenna 2.12, we can obtain the values of the antenna dimensions[19]

$$W = \frac{c}{2f_r}\sqrt{\frac{2}{\epsilon_r + 1}} \tag{3.1}$$

$$L = \frac{c}{2f_r\sqrt{\epsilon_{eff}}} - 0.824h(\frac{(\epsilon_{eff} + 0.3)(W/h + 0.264)}{\epsilon_{eff} - 0.258)(W/h + 0.8)}) \tag{3.2}$$

Where h is the height of the substrate ϵ_r is the dielectric constant of the substrate, ϵ_{eff} is the effective dielectric constant determined as (3.3), and f_r is the operating frequency of the application, in our case 3.6GHz

$$\epsilon_{eff} = \frac{\epsilon_r + 1}{2} + \frac{\epsilon_r - 1}{2}[\frac{1}{\sqrt{1 + 12(\frac{h}{W})}}] \tag{3.3}$$

Since these operations are quite simple, there are a,lot of online calculators[24] that will provide the dimensions of the patch easly.

3.1.1.1 Choice of material

The first objective of the project is to find the best substrate material available in the laboratory for our application. In order to find the best substrate a comparison between the following features will be made: The efficiency, small dimensions, a small sensitivity to changes and able to match at 50Ω. The final comparison will be made in the following 4 substrates: ROGERS4003, FR4, TRF45 and CUCLAD as

Each of the previous formulas were applied with the height and the dielectric constant for every subtract to obtain the approximated dimensions. They were corrected until the minimum reflection coefficient was exactly at 3.6GHz as can see in Table 3.1. The simulation precision was not that precise, since the mesh (the triangles in which the area of the model is divided), were big. This was done because the main goal, was not to find the exact value of the simulation, but compare the materials and make the simulations quick.

Substrate	Dielectric constant	W(mm)	L(mm)	h(mm)	Feeding point(mm)	Tangent loss
ROGERS4003	3,38	28,14	20,5	1,52	10	0,0027
TRF45	4,5	25,11	16,8	3,05	8	0,0035
FR4	4,5	25,11	17,75	1,5	7,5	0,03
CUCLAD	2,17	33,9	25,6	1,6	11,75	0,00009

Table 3.1: Dimensions and features for each substrate patch antenna designed

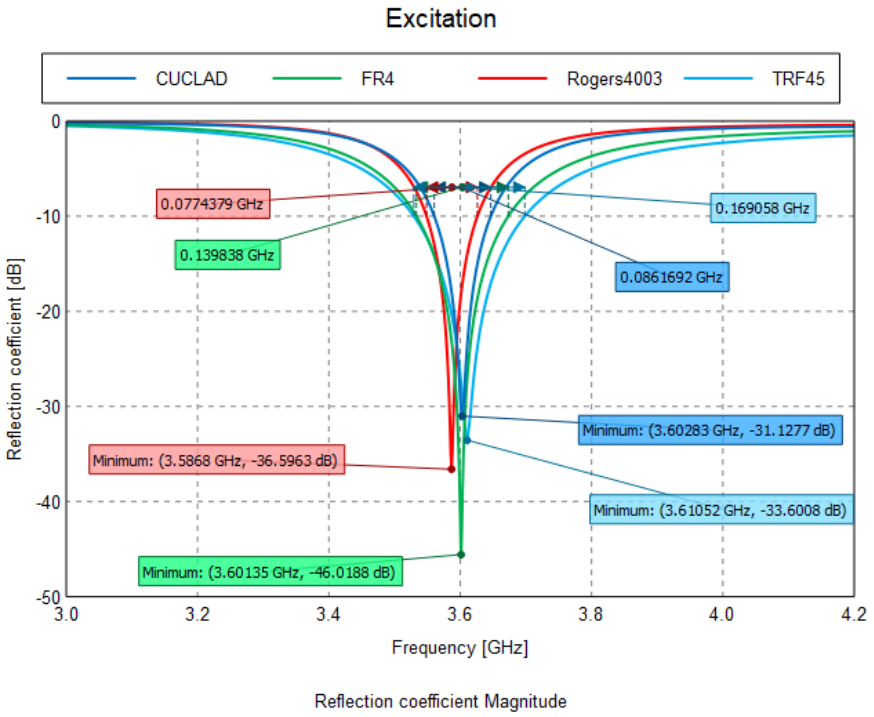

Figure 3.1: Reflection coefficient of the patch antenna designed with different substrates

.

As we can see in the Figure 3.1, we have matched correctly all the substrates at 3.6GHz with a narrow bandwidth at -10dB between 86MHz and 160MHz. This means that a well matched antenna to 50 Ω can be obtained with all the materials (with its height,dielectric constant and tangent loss) with the correct feeding point and the correct dimensions.

Although all the materials could have been used, it is important to remark that the TRF45 substarte, suffers a remarkable variation of the operating frequency(100MHz), if the dimensions have a minimum change of 0.1mm.

Another fact to take into account is that not all the materials have the same efficiency. Even though the efficiency is not the main feature of patch antennas, it is important to have the maximum efficiency

of transmission, since we don't want to lose power in any application. By making a comparison of the different patch antenna efficiencies depending on the substrate they use in Figure 3.2, we see that in the case of FR4, is much lower due to the tangent loss intrinsic of the material. Just a 0.39 compared to the 0.76-0.89 that the others materials have. This will exclude this material from the selection. It is important to see that in the Rogers4003 patch antenna, the efficiency goes up from 1, this is caused because FEKO would need more frequencies to converge the results.

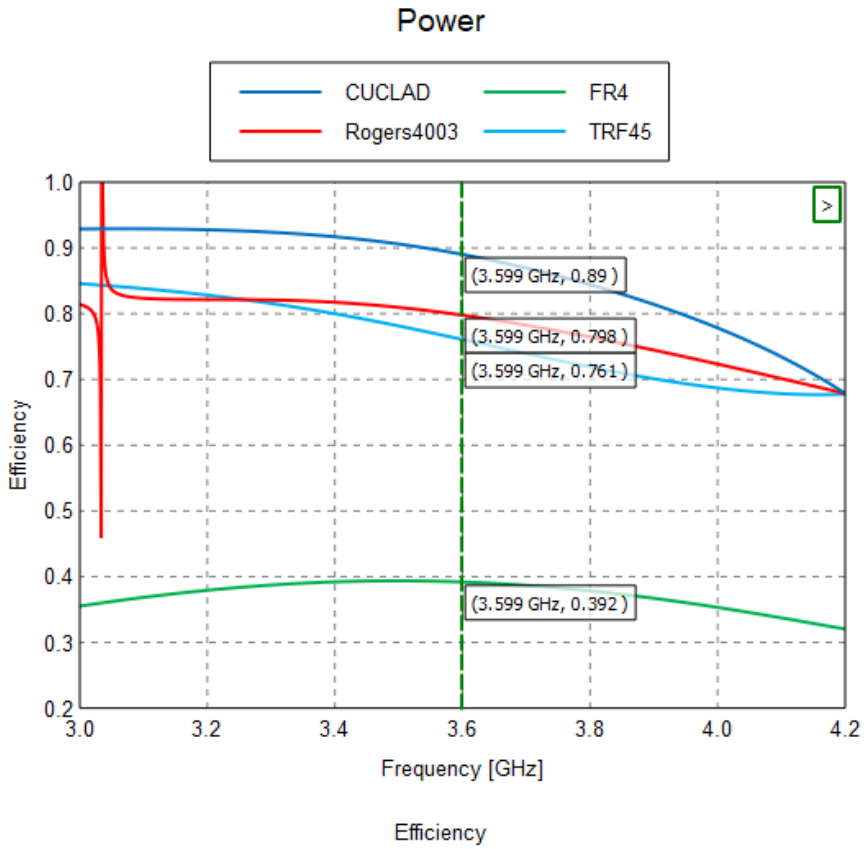

Figure 3.2: Efficiencies of the different patch antennas

.

Being left with just two materials, ROGERS4003 and CUCLAD. This two materials have both a similar efficiency and a good sensitivity to fabrication errors. So we have to take another variable in the decision, the size allowed by the substrate. As we will see in Chapter 5, the antenna spacing is a key to obtain degrees of freedom in a MIMO transmission, so the most spaced they are, the better our transmission will perform. Given this feature, we want the smallest antenna. The patch antenna that fullfil best the requirements is the one with ROGERS4003 as a substrate, since it is 5mm smaller in each axis, this will mean a 20mm increase on the spacing to the 270x90mm board that will hold the array.

The final conclusion as seen in Table 3.2 the best substrate choice is be the ROGERS4003 which although not the best choice in any of the features. It offers the best dimensions in contrast with the

patch performance. It has a good efficiency compared to the FR4 and although it is susceptible to fabrication errors, the precision of the milling machine can allow us this certain margin.

Material	Sensitivity with 0.1mm error in L dimension	Dimensions	Efficiency
ROGER4003	1.5%	20.5x28.14mm	79.77%
FR4	0.7%	17.75x25.11mm	39.18%
TRF45	2.7%	16.8x25.11mm	76%
CUCLAD	1%	25.6x33.9mm	89%

Table 3.2: Choice of material

3.1.2 Array of 4 antennas

Now that the material of the antenna has been settled. The final deign of the array will be made. In this scenario we have to design the 4 patch antenna on a 270x90mm board, which is the maximum our milling machine is able to support.

Before starting with the design it is important to select, in which position the antennas will be. In order to increase the maximum separation between antennas the most logical way to do it is to do it in the orientation that will be named "A" seen in Figure 3.3. However it is important to notice than in mode TM_{010} the fields generated in the L edge cancel each others making a non-radiating edge, while the W edge operates as the radiating slot. This fact causes that the orientation "A" seen in Figure 3.3, the patches are not as isolated as in the orientation "B" seen in Figure 3.4. Since patches isolation is something we want to accomplish in order to have the maximum power radiating and not entering the lateral patches, the orientation chosen is the symmetrical one.

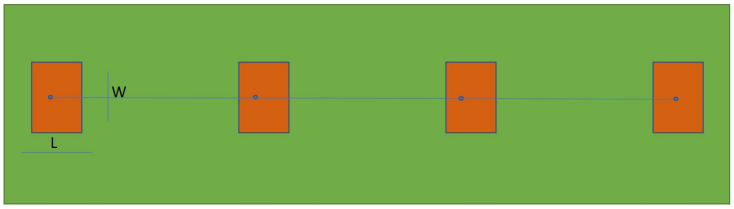

Figure 3.3: A orientation

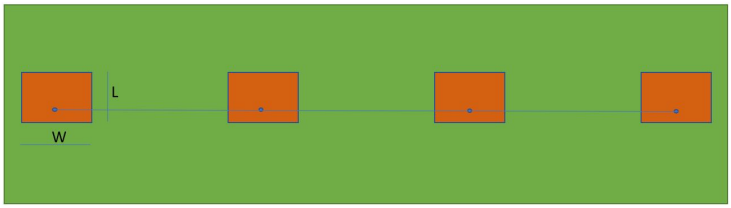

Figure 3.4: B orientation

With the orientation of the patches established, the ROGER4003 as the substrate material and cooper as conductor material we are ready to start designing our array.

Since a fine mesh simulation in this exact model can take long (1-2 hours each simulation) it is important to be sure about the changes done in the model compared to the model with just 1 antenna. At the same time have an approach to determine the best dimensions for the array.

The dimensions of the antenna and the array board of 290x70mm allows us to consider two different separation between antennas: 0.75λ and 1λ. Meanwhile the 0.75λ configuration will have a most similar radiation diagram for exterior and interior patches, making the system more predictable, since all would be the same with the same values of power. The 1λ configuration could have less similar radiation patter since the exterior patches are closer to the edge and this could "curve" the radiation diagram due to the fringing effect[1]. However, since the patches are further from each other the isolation between them would be better and the singular values of the MIMO transmission can be easier obtained with larger separation. This comparison will be made meanwhile the array matching is done.

Once the matching is done and we have a reflection coefficient around -15dB-30dB we will consider that the antenna is well matched, and ready to execute the most heavy simulation with fine mesh, but reducing the number of frequencies to measure to 22 so the simulation doesn't take 1 full day.

The final dimensions of the patch antennas are the same as 3.5 following:

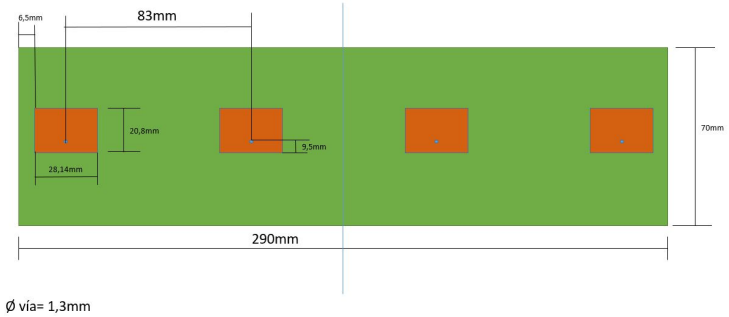

Figure 3.5: Final patch dimensions

[1]Effect that considers the field as not closed to the cavity, and with the edge closer, some fields could not be fitted inside the cavity

- Length=20.8mm
- Width=28.14mm
- Feed point= 9.5mm from the centre
- tangent loss=0.0027

From now on we will consider patch 1 and 4 as the outer patches while the patch 2 and 3 will be the inner ones as in Figure3.6. The comparison of the reflection coefficient and the S parameters between the two configurations will be made in the Figures 3.7 and Figure 3.8:

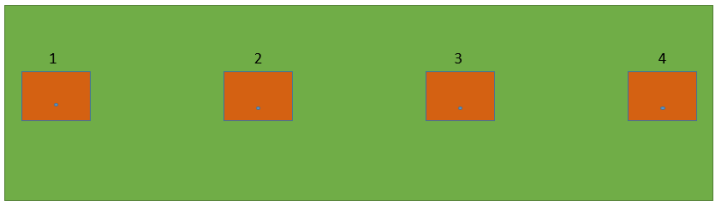

Figure 3.6: Patch enumeration

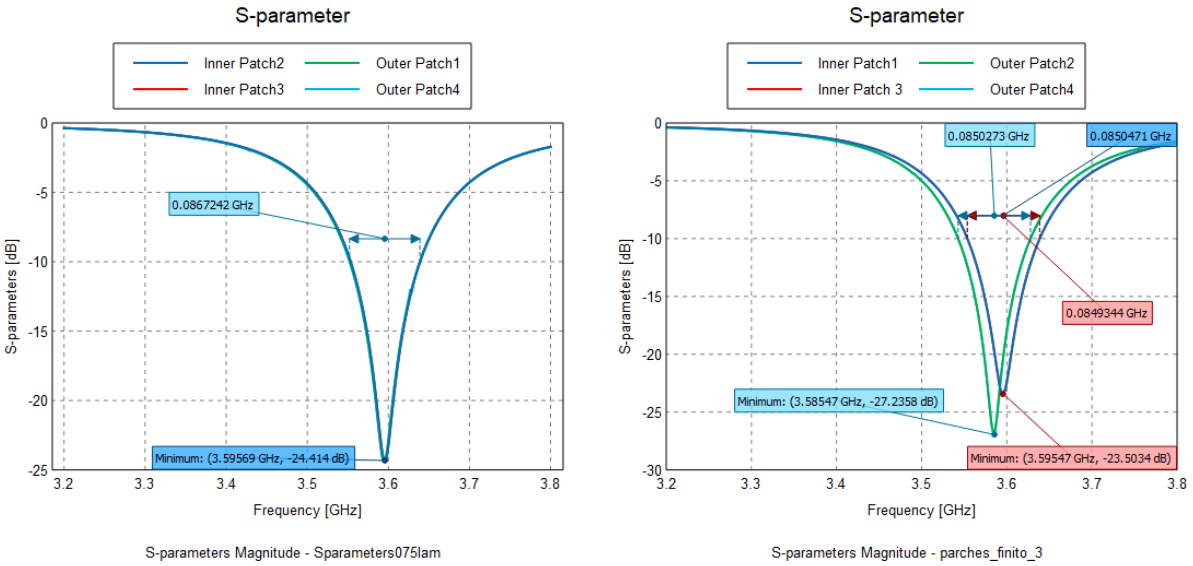

(a) reflection coefficient in 0.75λ separation

(b) Reflection coefficient in 1λ separation

Figure 3.7: Reflection coefficient in different patch separation

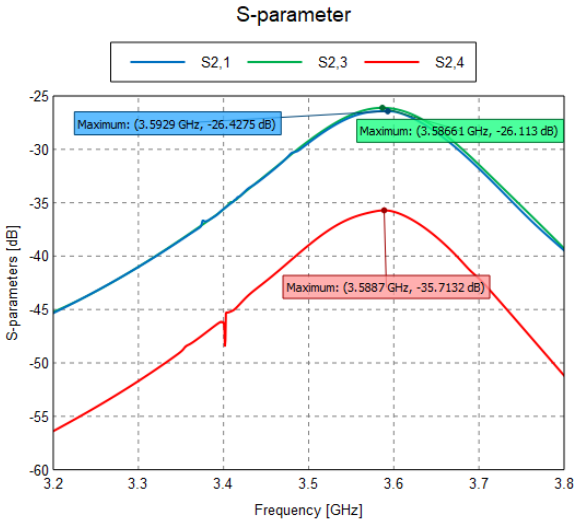

(a) S-paramaters patch 2 in 0.75λ separation

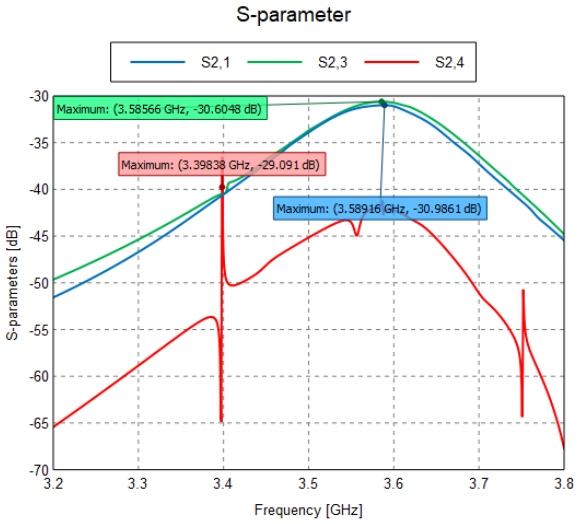

(b) S-paramaters patch 2 with 1λ antenna separation

Figure 3.8: S-parameters between inner patch 2 with different patch separation

Here we can clearly see what was expected from both of the configurations. In 0.75λ the outer patches are far enough from the edge, that it will no affect the radiated field, making the reflection coefficient really similar to each other as seen in figure 3.7b. It can also be seen that, since in TM_{010} the W edge is the one radiating, the interaction between antennas is minimal since the side in parallel is L side. In figure 3.8a we see how the attenuation suffered from radiated power in patch 2 and received in patch 1 and 3 is really similar. Clearly, it can be seen that the two antennas at the same distance will have very similar value of attenuation of 26dB at the receiving patches 1 and 3, while patch 4, that is the one further away (2 times the separation, the red one), will have a more attenuated signal, 35.7dB

If we now compare this results to the 1λ configuration, we will see that in this case, the values of the reflection coefficient in the outer and inner patches are a bit different 3.7a. This is caused by the fact that the outer patches are closer to the edge of the board. This causes that with the same dimensions, the matching is not the same in the inner and exterior patches. However, in both patches, the working frequency is around the 3.6GHz within a range of 77MHz. On the other side, since the patches are more separated from each other the isolation from the patches is better as seen in 3.8b, where the attenuation of the signal in the nearby antennas is around -31dB and the further one is around -42dB.

Focusing on the radiation patter and the E,H planes we will also see this difference between the two separations array that have been explained before.

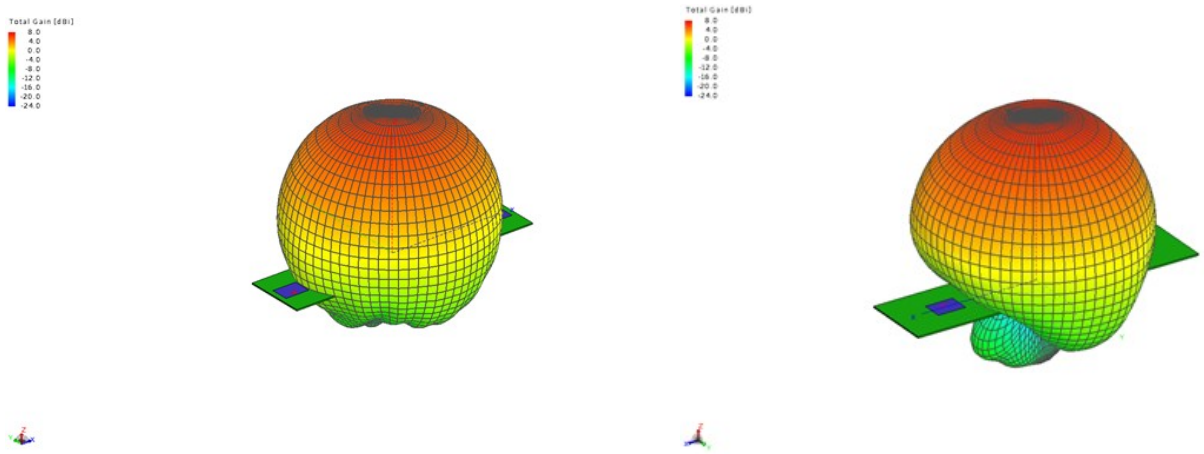

(a) Outer patch antenna separated 1λ (b) Outer patch antenna separated 0.75λ

Figure 3.9: Radiation pattern of the outer patches

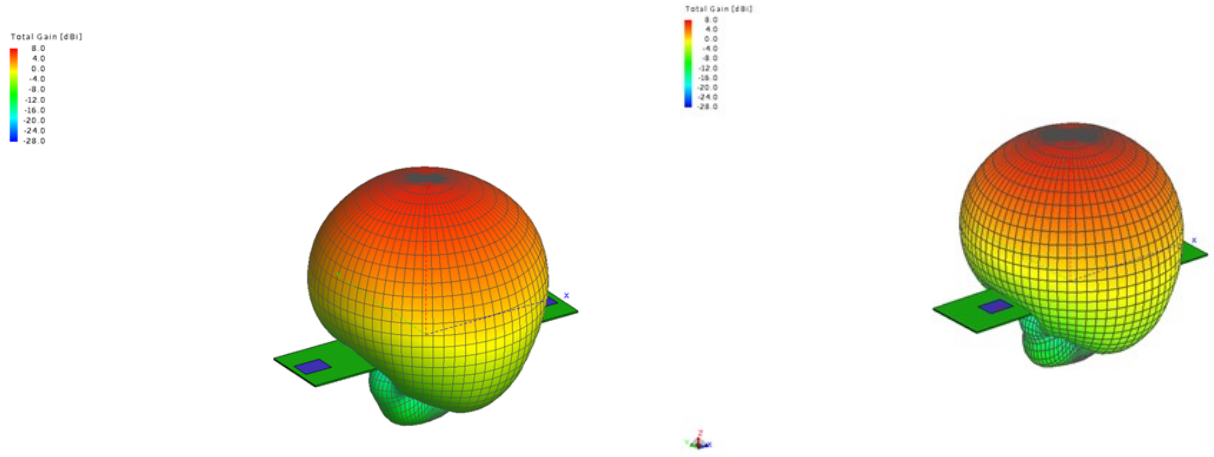

(a) Inner patch antenna separated 1λ (b) Inner patch antenna separated 0.75λ

Figure 3.10: Radiation pattern of the inner patches

A visual representation of the radiation pattern that would have the different patches of the array depending on the configuration is represented in Figure 3.9 and Figure 3.10. If a comparison is done, the inner patches would have basically the same pattern independently of the separation between the antennas of the array as is seen in Figure 3.10 where the patterns have basically the same form and the same power distribution. However, in the outer patches this comparison changes. The outer patch of the array separated 0.75λ has the same pattern as the inner ones as we can see in Figure 3.9b, the outer patch of the array separated 1λ seen in Figure 3.9a has a bit different pattern. Especially in the surface of the board and in the back of the antenna. As has been said before this is due to the fact that in the case of separating the antennas 1λ, the space to the edge of the board is minimum. This makes this

change of form on the radiation pattern. Even though the pattern is different we will see in the following pictures, that since in our MIMO transmission application the angles that will be used are between $-60°$ and $60°$), this difference is not the most influential.

To see clearly which are the exact differences in the radiation pattern, we can use the H, and E planes. This planes represent the radiation pattern in one coordinates axis plane. In this case the colour blue lines represent the representation in inner patches, meanwhile the green ones are for the exterior ones.

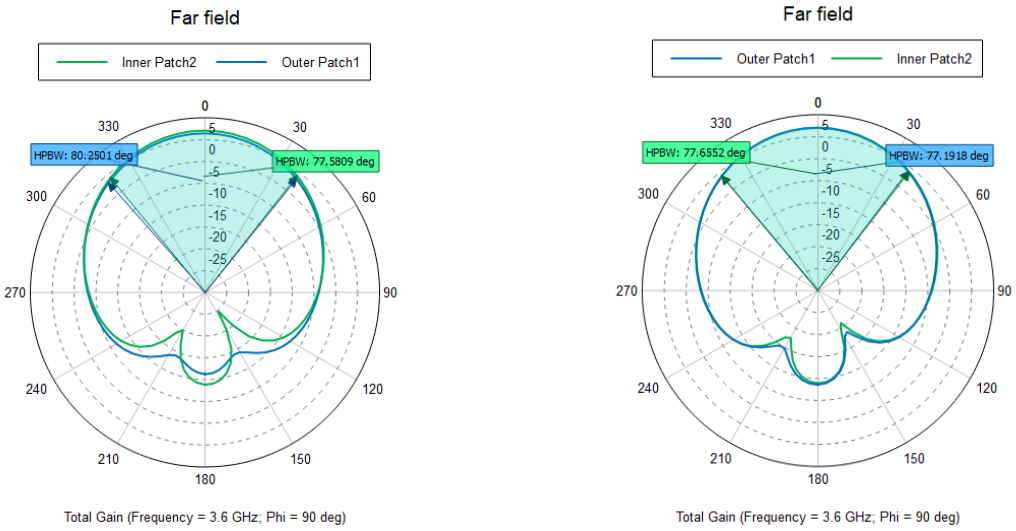

(a) E-plane for array separated 1λ

(b) E-plane for array separated 0.75λ

Figure 3.11: E-planes for different configurations

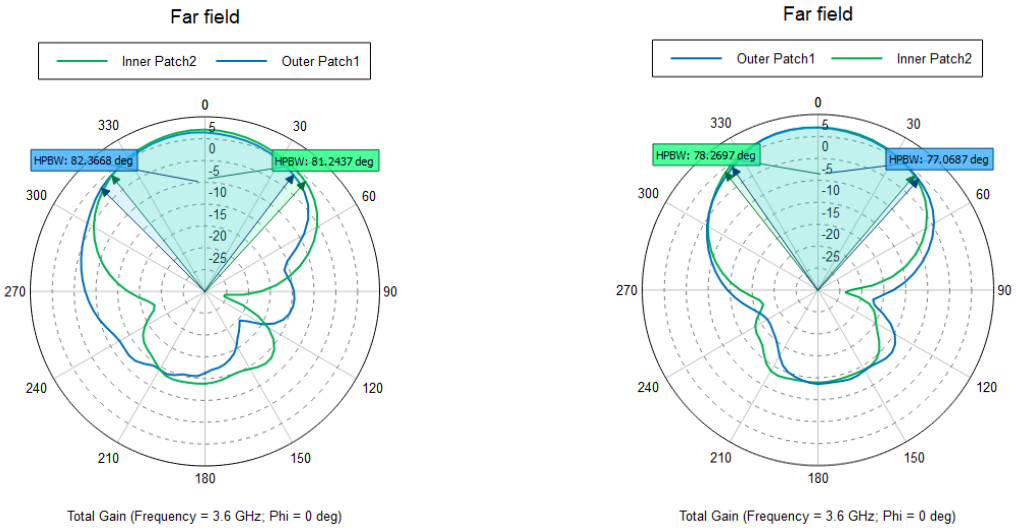

(a) H-plane for array separated 1λ

(b) H-plane for array separated 0.75λ

Figure 3.12: H-planes for different configurations

As we can see in Figures 3.11 and 3.12. The planes comparing the E-plane inner and outer patches 3.11b, with the space between antennas as 0.75λ is basically the same. It just start to get a bit different in the back radiation of the antenna. Especially on the nulls situated at 150° and 210°. However, in our case it is not important since we don't want to radiate backwards. In the same E-plane but with the space between antennas being 1λ 3.11a, the pattern is basically the same, but with a steeper difference at the rear part of the antenna. It starts this difference at 120°. The half power bandwidth is situated in both cases in the range of $-80°$ and 77° meaning that in a range of 157° the transmitted power will not be halved.

In the H-plane the situation will be quite similar but with a more abrupt differences between the patterns as is seen in 3.12. In the separation of 0.75λ 5.1.5. Both patterns are equal in the front lobe, but in the 60° they start to differentiate. Not in an abrupt way but have minor differences along the pattern that will have to be considered for the applications the antennas are used to. In the same way as in the E-planes, the configuration of 1λ, have a similar pattern than the previous one, but with the difference more pronounced, specially on the outer patch due to its proximity to the edge of the board.

With all this data that we have collected with the comparison between the two arrays. The final decision is to make an array with 1λ of separation seen in Figure 3.13. Even though the radiation diagram of the inner and outer patches are different, the front lobe of the pattern is equal enough to consider that when the 4 patches radiate will create a similar pattern in front so the receiver can receive the maximum power of the transmitter. At the same time we will gain some space that could help us to have an additional degree of freedom in the MIMO transmission.

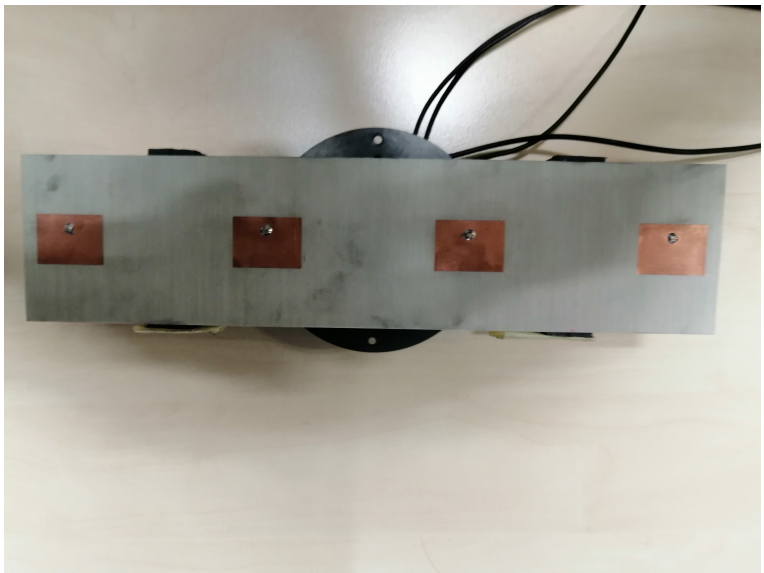

Figure 3.13: Fabricated antenna

3.2 Measurement

Once the antenna is fabricated, a comparison of the results to the simulation has to be done in order to be sure that the simulation is well done.

We will divide this measurement is 2 different parts:

- Network analyser: This measurement will be made to make sure that the 4 patches are well matched and isolated. The extraction of the S-parameter will be made here
- Anechoic chamber: In the anechoic chamber the measurement of the radiation pattern of the antenna will be made. At the same time we will do a breve explanation of how the anechoic chamber works, and how to obtain the values of the gain/efficiency will be considered.

3.2.1 Vector network analyser

Once the antenna is built, what we will do first of all is to measure its S parameters with a VNA vector network analyser.

To do this, we will first calibrate the 4 ports of the VNA with an electronic calibration at 50Ω. To calibrate it is better to take into account how we will measure the antenna, and in which position the antenna will work. In our case this position will be in parallel to the ground. Finally connect each of the 4 ports of the network analyser with the respective e patch of the array.

Once connected we will be able to see all the different S parameters of the real antenna 3.14:

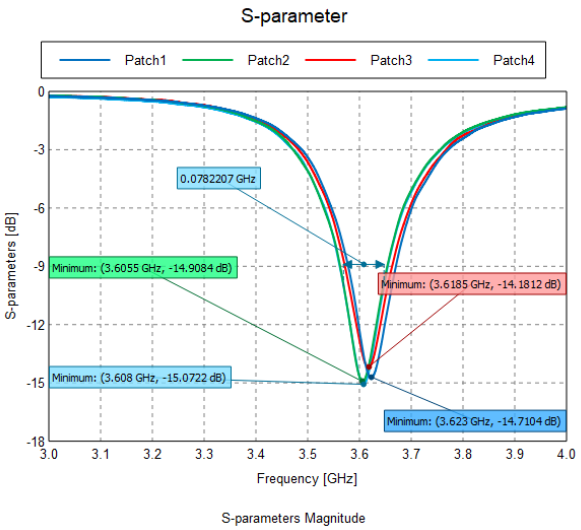

Figure 3.14: S-parameters measured in the network analyser

In this image we clearly see how the matching of the antenna (S11, S22, S33, S44) is a little shifted **(10-30MHz)** compared to that of the simulations. The minimum of the reflection coefficients is not as

low as in the simulations, since in this measurement they are aroud the -15dB, while in the simulation they are around the -30dB. Next, we will make a patch-by-patch comparison with the simulations and measurements with the VNA in order to know exactly which has been the shifting and if it is too much for our application.

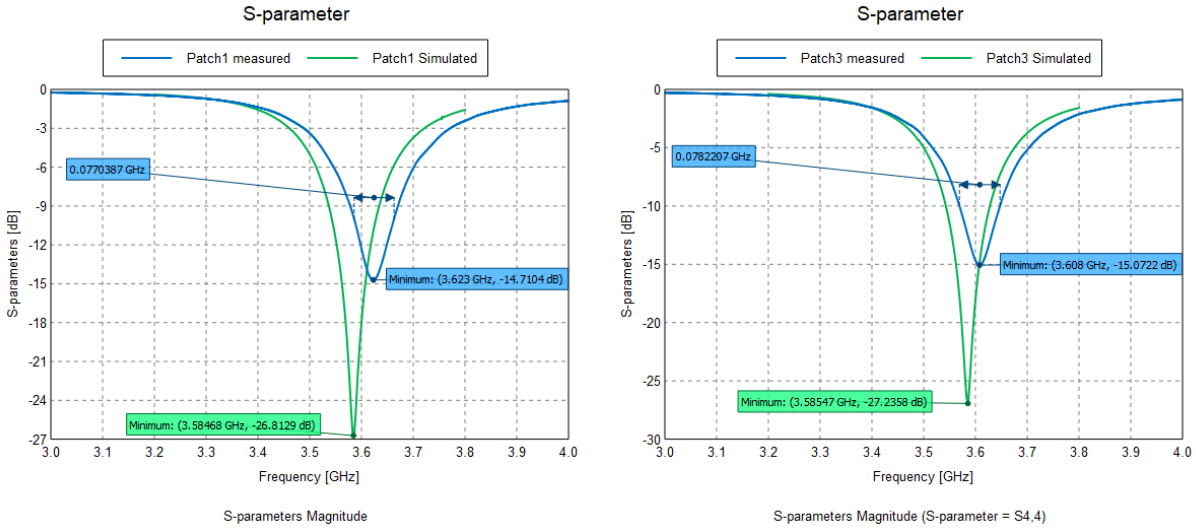

(a) Outer patch 1

(b) Outer patch 4

Figure 3.15: Outer patches comparison simulation vs network analyser

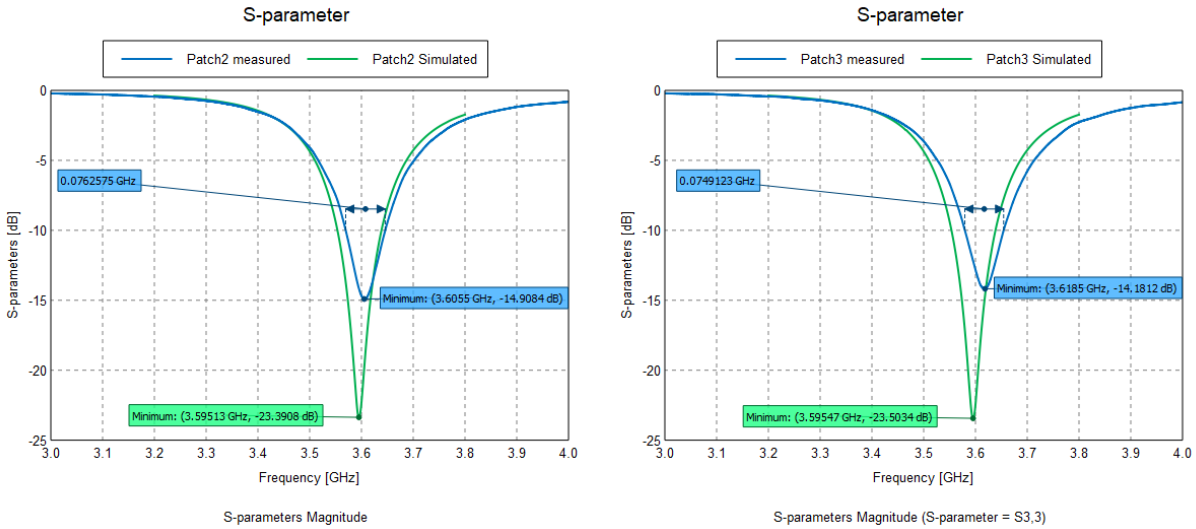

(a) Inner patch 2

(b) Inner patch 3

Figure 3.16: Inner patches comparison simulation vs network analyser

Shifting in frequency and its percentage:

- Outer patch 1 Figure 3.15a: 40 MHz shifted to higher frequencies, 1% of the total frequency
- Exterior patch 4 Figure (3.15b): 23 MHz shifted to higher frequencies, 0.65% of the total frequency
- Inner patch 2 Figure (3.16a): 14 MHz shifted to higher frequencies, 0.4% of the total frequency
- Inner patch 3 Figure (3.16b): 17.5 MHz shifted to higher frequencies, 0.5% of the total frequency

It should be noted that in the case of the simulations, as expected due to the symmetry, the interior patches had the same reflection coefficient while the exterior patches, although different from the interior patches, also had the same. In these measurements this does not happen, but each patch has a different reflection coefficient. Which we will analyze below to what may be due.

In any case, we can highlight that the 3.6GHz working frequency is always within the bandwidth margin of -10dB that can ensure a radiation efficiency of 90%.

The possible factors that can influence this changes are the following:

- Imperfections in the milling of the ROGERS4003. In the width dimension (W) of the substrate there is a margin of error of $\pm$ 1mm
- The antenna separation is 83.43mm instead of the 83.33mm which should be the lambda dimension at 3.6GHz.
- The one that is likely to affect the most, there is an uneven (very small) groove around the copper of the antennas due to milling (copper extraction). This groove varies the relative dielectric constant of the system (reduces it) causing the relative wavelength to decrease. This causes the antenna to become a bit out of adjustment and the operating frequency to increase (possible cause of this shift at higher frequencies). On the other hand, as each antenna is uneven, it can have a different frequency shift and mismatch.

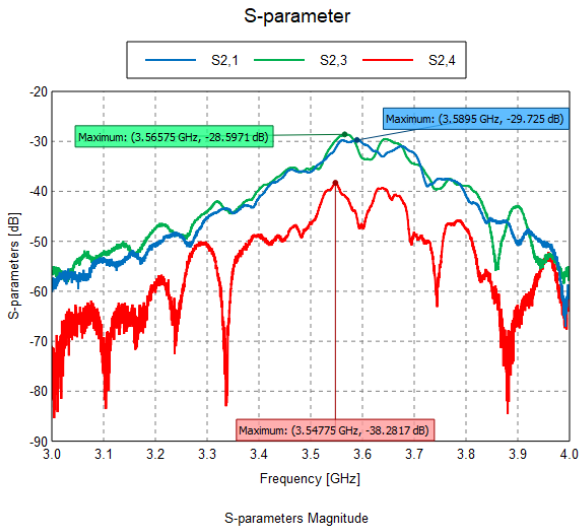

Figure 3.17: Measure of isolation of patch 2

Taking a look into the antenna isolation, represented in the S-parameter on the first inner patch as S21, S23, S24, we will see in Figure 3.17. The signal level received by the closest antennas (1 lambda separation) is attenuated 30 dB with respect to that transmitted by the reference antenna 1, while the antenna that is at a distance of 2 lambdas receives the attenuated signal 38 dB. Comparing it to the Figure 3.8b the values measured are really similar to the ones simulated.

It should be noted that the frequency shifts measured are about 0.4-1% from the ideal operating frequency of 3.6GHz. In our case and because the operating frequency is within the -10dB bandwidth it does not cause us great problems. The final consideration is that even though the simulation and the measurement doesn't match exactly, MIMO transmission can also be done in good condition.

3.2.2 Anechoic chamber measurement

In the characterisation of the array . The transmitting antenna will be a cylindrical probe that operates in the S-band (2.6-3.9GHz).

On the other side, our antenna array, will receive in just one of the four ports, and the rest will be loaded with 50Ω so the characterisation of one patch can be made. It is important that the power of the transmission is the same in all the measurements of the different ports so the comparison can be made. In order to make sure that the position of the antenna is the exact one, we will rotate the transmitting antenna until we are receiving a minimum at 3.6GHz. This position means that the antennas are polarisation is orthogonal. All the antennas of the system will have some pieces of carbon doped below and above, so the radiation doesn't reflect with the metal.

The configuration of the measurement is the following

- Frequencies: From 3.5GHz to 3.7GHz in 5 steps (0.5GHz/step).
- Azimuth axis: From $0 - 170°$, avoiding the 180° sinc it would overlap with the 0. Steps of 10°.
- Elevation axis: From $0 - 80°$ in 10° steps so the full radiation diagram can be represented.

Once we have all the patches measured in the anechoic chamber what we will do is compare them with the simulations that were done with their time in FEKO in order to be able to determine if the results and simulations are similar. At the same time we can appreciate in more detail what are the exact measurements of the different parts of the array.

In order to transfer the data obtained in the anechoic chamber to FEKO to compare the results, the MATLAB function "$asysol2fekoffe$"A.1 will be used. Its function is to read the file from the anechoic chamber software, and transform the data to a text file format that FEKO is able to read.

The outer patches will be the first ones to be analysed. First of all we will make a small comparison of the measurements of plane H 3.18a and plane E 3.18b with the measurements made with higher quality (steps of 5 degrees).

Next we will look in a polar diagram the differences of the different planes:

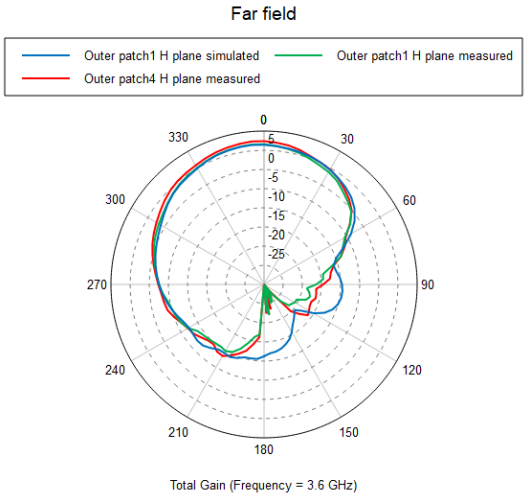

(a) H plane comparison outer antennas

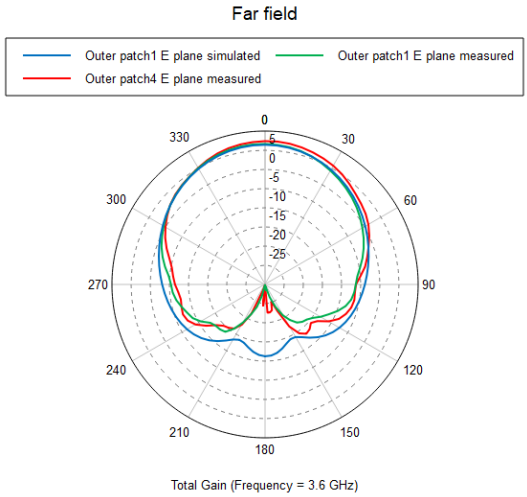

(b) E plane comparison outer antennas

Figure 3.18: Outer antennas planes comparison between simulation and measurement

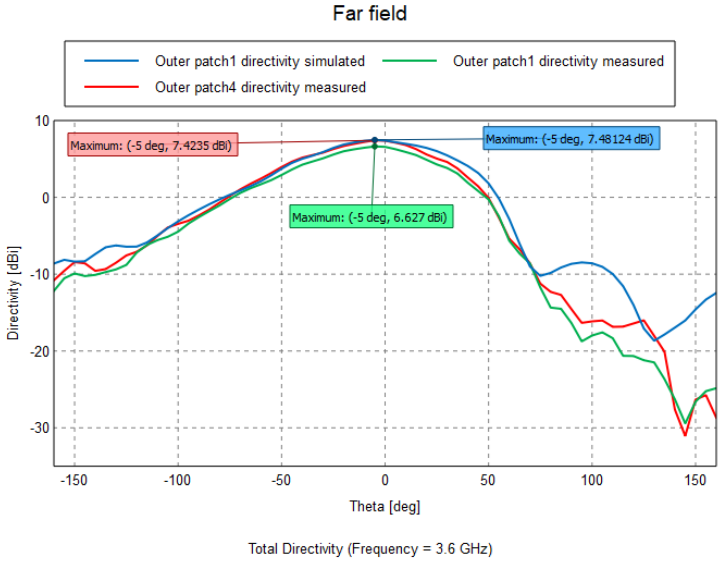

Figure 3.19: H plane outer antennas directivity comparison

It is important to note, that to compare properly the symmetrically situated patches, the axis was rotated 180°, so the fields were in the same direction.

In this case we can see in Figure 3.18, as especially in the main angles of the front lobe (-120.60), the results are very similar between the simulation and the two patches. Where these small variations may be due the antenna fabrication is not exactly as in the simulation or that even the absorber above and below the antenna is not perfect symmetrically placed. On the other hand, the angles at the antenna may be more different because both the positioner and the masts were not considered in the simulation and

may add asymmetries to the measurements. As for the maximum measure of directivity, we see in figure 3.19 that it is very similar in all three cases and will be analysed later when calculating the efficiency of each patch. We see how they clearly remain very similar shapes until the rear angles intervene.

As for the inner patches, the condition is very similar Figure 3.20. In this case, when we take a look at the differences between the measurements and the simulations, we notice a change at the farthest angles. If we look more closely at the two planes in Figure 3.20a and Figure 3.20b, we can see how the above statement is confirmed. Where the main angles have very similar values but the ones behind the antenna differ quite a bit due to the lack of isolation between antennas.

Although the shape and values of the directivity Figure 3.21 of the diagram between the angles -65 to 65 remain very similar. And the maximum point located at 0 degrees with a value very close to 8dB, while the differences are below the -30dB. This means that the measurement and the simulation have basically the same directivity.

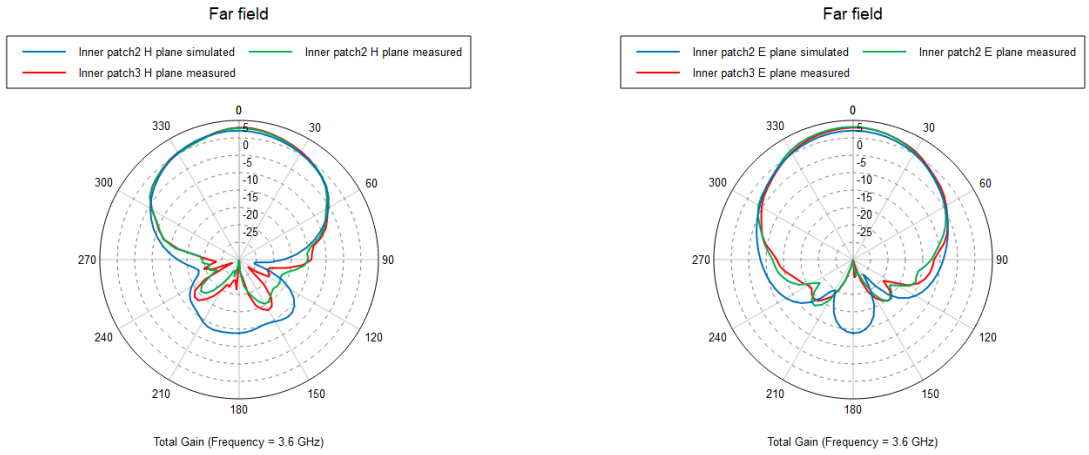

(a) Inner antennas H plane comparison

(b) Inner antennas E plane comparison

Figure 3.20: Inner antennas planes comparison between simulation and measurement

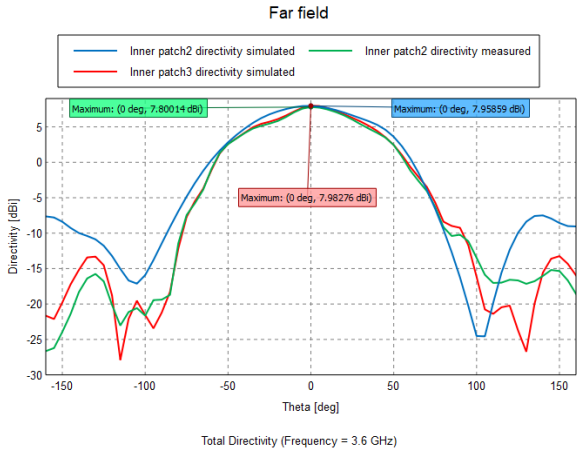

Figure 3.21: H plane inner antennas directivity comparison

To end this section the only proof that our simulation is close enough to the reality is the efficiency of the antenna. The efficiency is determined by the relationship between the power radiated by the antenna and the power delivered to the antenna, which we will identify as the gain of the antenna and the directivity of the antenna.

The gain of each patch will be obtained by the measurements made in the anechoic chamber,comparing the gain of the system with the patches and one reference antenna. The antenna selected needs to work at 3.6GHz so the receiver has the same performance. In our case, was the Standard Gain Horn WR284 antenna that has a gain of 17.95dB AT 3.6GHz. In this case, the signal level difference between receiver and transmitter is -0.6dB. With a simple difference of the measurements we can extract which is the gain of each patch.

The directivity of the antenna will be obtained by integrating the normalised measured radiation pattern that is what the function "$asysol2fekoffe$"A.1 does.

Making the final Table3.3 as:

	Measurement			Simulations		
Patch	Gain	directivity	efficiency	Gain	directivity	efficiency
Patch1	5,95	8,5	0,5542	6,5	7,4	0,6919
Patch2	6,55	9,1	0,5444	7	7,9	0,7767
Patch3	6,85	9,4	0,5440	7	7,9	0,8023
Patch4	6,25	8,5	0,5856	6,5	7,4	0,6969

Table 3.3: Efficiency comparison

Although the efficiency of the antenna is around the 50-60% and the simulated antenna was around the 70%-80%. This differences can be due errors in antenna fabrication or errors in the simulation due to precision.

As a conclusion, we can say that the designed and measured array, although different, satisfies our requirements so it will be used as a transmitter in our MIMO application together with the FMCOMMS5-EBZ evaluation board.

Chapter 4

Theory behind MIMO

In this chapter we will discuss which are the basic properties of a time-invariant wireless channel with multiple transmit antennas n_t and multiple receive antennas n_r. MIMO properties are given by the channel matrix H, which represents the relation between the transmit and receive antennas. We will show how this configuration allows us to increase the capacity of the channel and therefore, transmit/receive more data.

4.1 Problem approach

We can describe a time-invariant channel[2] of Figure 4.1 as (4.1):

$$y = Hx + w \tag{4.1}$$

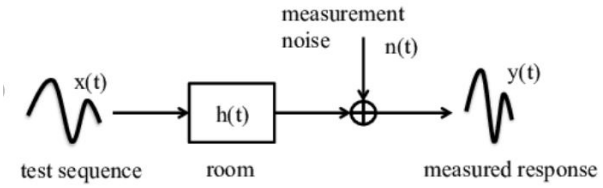

Figure 4.1: Time-invariant channel

Where x represents the transmitted signal from the n_t antennas (vector of 1 x n_t),y is the received signal from the n_r antennas (a vector of n_r x 1), and w is the white Gaussian noise. H is the deterministic matrix of our channel (n_r x n_t), each element of H represents the gain between the transmit antenna i and receive antenna j[2].

From this matrix H the capacity of the channel can be obtain by decomposing it into a set of parallel, independent scalar sub-channels. To do so a basic linear algebra is applied; a rotating operation U, a

scaling operation Γ, that will be named S from now on, and another rotation operation V thus obtaining the singular value decomposition of matrix H (SVD)[2] (4.2):

$$H = USV^* \tag{4.2}$$

Matrices U and V are unitary[25], they have dimensions the dimensions of n_t x n_r. Matrix S is a rectangular matrix of n_t x n_r whose diagonal elements are non-negative real numbers and whose off-diagonal elements are zero an represents the singular values of matrix H. The number of singular values of the matrix S will be the minimum number of transmit or receive antennas $n_{min} = min(n_t, n_r)$. Each of this values will be the voltage gain of the parallel independent sub-channels, so, the sum of squares will be the power gain of our system.

$$H = \sum_{i=1}^{n_{min}} \lambda_i u_i v_i^* \tag{4.3}$$

Figure 4.2 shows a schematic version of (4.3)

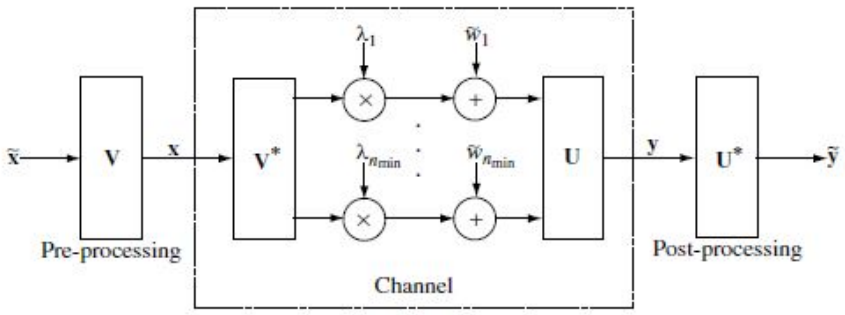

Figure 4.2: Converting MIMO channel into a parallel channel through the SVD[2]

If we define [2]:

$$\tilde{x} = V^* x \tag{4.4}$$

$$\tilde{y} = U^* y \tag{4.5}$$

$$\tilde{w} = U^* w \tag{4.6}$$

We can rewrite (4.1) as 4.7:

$$\tilde{y} = S\tilde{x} + \tilde{w} \tag{4.7}$$

In Figure 4.2 we can identify 3 different steps:

1. Preprocessing signal: It consist on multiplying the transmitted signal with the rotation operation V:

$$x = V\tilde{x} \tag{4.8}$$

   Notice that this rotation, in the first instance will not produce any result from which we can obtain any conclusion

2. Channel transmission: The first step is make to multiply by V^*, so it will cancel(thanks to the unitary matrix properties) with the previous matrix V giving us only the transmitted signal. Finally making the product of this signal the scalar factor with some noise added and multiplying by the rotation operation U, obtaining:

$$y = U(S\tilde{X} + \tilde{w}) \tag{4.9}$$

3. Postprocessing: The final step is, once the signal is received, rotating it again with the matrix U^* that will cancel with the previous U from the channel transmission. This procedure will directly gave us the received signal from the transmitted signal.

In case we wanted to prove that our system is correct, we could obtain the transmitted signal from the transmitted signal and all the transformations

$$\tilde{x} = S^{-1}U^*HV\tilde{x} \tag{4.10}$$

Note that this singulars values will determine the number of sub-channels we can obtain. This will divide our transmission in n_{min} number of channels that can be used for n_{min} multiusers transmissions.

The capacity C is the parameter that defines the maximum rate at which information can be transmitted through a channel[26]. It is defined by the signal to noise ratio of the channel, in how many subchannels we are able to divide the principal channel, and how many voltage gain is in each subchannel.

To determine the performance of the transmissions, it is important to divide into two different scenarios:

- High *SNR* (signal to noise ratio): The idea in this scenarios is to allocate equally the amount of power in each independent sub-channel so the capacity of our channel would be [2]:

$$C = klogSNR + \sum_{i=1}^{k} log(\frac{\lambda_i^2}{k}) \;\; bits/s/Hz \tag{4.11}$$

  Where k is the number of singular values of channel H and *SNR* is the relation between signal power and noise power.

- Low *SNR*: At low *SNR*, the optimal policy is to allocate power only to the strongest singular value,[2]

$$C = \frac{P}{N_0}(max\lambda_i^2)log_2e \;\; bits/s/Hz \tag{4.12}$$

4.2 SIMO & MISO

We have seen all the basic information obtain from a channel is given by matrix H. It is important to remark that in this project, all H matrices will be considered time-invariant.

Let start by obtaining the H matrix of the single input and multiple output system SIMO of Figure 4.3

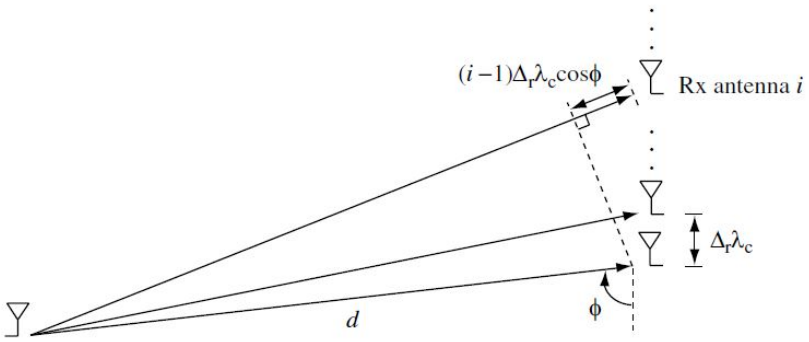

Figure 4.3: SIMO transmission[2]

In this case the considerations are:

- Free space
- The antenna separation at the receiver array is $\Delta_r\lambda_c$ where Δ_r is the normalised separation between received antennas and λ_c is the wavelength of the carrier.
- The dimension of the antenna array is much smaller than the distance between transmitter and receiver d.

- The receive antenna array has $n_r antennas$.

Giving the relation between the transmit antenna and the different receive antenna of the array:

$$h_i = a \cdot exp(-\frac{j2\pi f_c d_i}{c}) = aexp(-\frac{j2\pi d_i}{\lambda_c}) \tag{4.13}$$

Where f_c is the frequency of the carrier, and d_i is the distance from the transmitter to each one of the antennas of the receiving array. This distance can be approximated (4.14), as the distance d which is the distance from the transmit antenna to the first receive antenna plus the increase of distance due to the antenna separation and the angle of incidence of the transmission ϕ.

$$d_i = d + (i-1)\Delta_r\lambda_c cos\phi \tag{4.14}$$

Then, we can rewrite (4.13) as matrix H (n_r x 1):

$$H = aexp(-\frac{j2\pi d}{\lambda_c}) \begin{bmatrix} 1 \\ exp(-j2\pi\Delta_r\Omega_r) \\ exp(-j2\pi\Delta_r 2\Omega_r \\ \vdots \\ exp(-j2\pi(n_r-1)\Delta_r\Omega_r) \end{bmatrix} = aexp(-\frac{j2\pi d}{\lambda_c})\sqrt{n_r}e_r(\Omega_r) \tag{4.15}$$

Where $\Omega_r = cos\phi_r$, since the signals received at consecutive antennas differ in phase by $2r\Delta_r\Omega_r$ due to the relative delay[2].

This scenario H is just a vector, so applying the SVD would allow just 1 singular value, so the sub-channel division could not be applied.

The MISO channel seen in Figure 4.4 with multiple transmit antennas and a single receive antenna is reciprocal to the SIMO channel. This means that transmit antennas are separated $\Delta_t\lambda_c$. The received signal of the channel will be defined by:

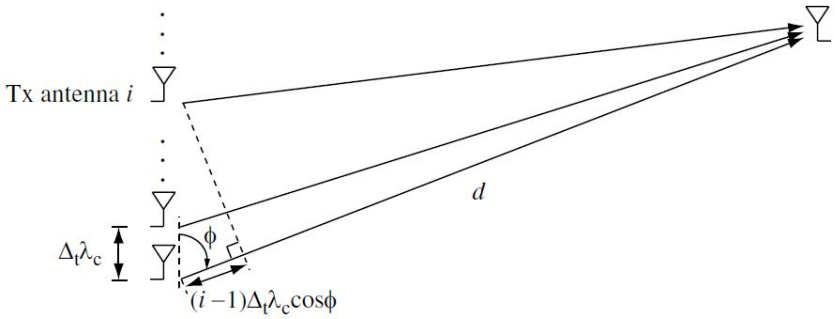

Figure 4.4: MISO transmission[2]

$$y = H^*x + w \tag{4.16}$$

Where

$$H = aexp(-\frac{j2\pi d}{\lambda_c}) \begin{bmatrix} 1 \\ exp(-j2\pi\Delta_t\Omega_t) \\ exp(-j2\pi\Delta_t 2\Omega_t \\ \vdots \\ exp(-j2\pi(n_t-1)\Delta_r\Omega_t) \end{bmatrix}^* = aexp(-\frac{j2\pi d}{\lambda_c})\sqrt{n_t}e_t(\Omega_t)^* \tag{4.17}$$

Where $\Omega_t = cos\phi_t$

As the concept is the same, with MISO transmission it's not possible to obtain more than 1 singular value. The power of the system can be increased with the number of antennas of the system, but not the number of sub-channels that can be obtained.

4.3 MIMO

Now that we the basic idea how the extraction of H matrix on MISO and SIMO transmission have been done. The only thing left to make a MIMO transmission is the combining of them.

To calculate the relation between each antenna of the transmission array and each antenna of the receiving array is just the same as (4.13), with the difference that in this case, H will not be a vector, but a matrix of $n_r x n_t$ elements.

$$h_{ik} = a \cdot exp(-\frac{j2\pi f_c d_{ik}}{c}) = a \cdot exp(-\frac{j2\pi d_{ik}}{\lambda_c}) \tag{4.18}$$

And so will be (4.14), since each transmitter antenna will have different paths between the receiving antenna i and the transmitting antenna k:

$$d_{ik} = d + (i-1)\Delta_r \lambda_c cos\phi_r - (k-1)\Delta_t \lambda_c cos\phi_t \tag{4.19}$$

Combining this formulas as we did in SIMO and MIMO transmissions we can extract the final H matrix:

$$H = a\sqrt{n_t n_r} exp(-\frac{j2\pi d}{\lambda_c}) e_r(\Omega_r) e_t(\Omega_t)^* \tag{4.20}$$

4.3.1 Geographically separated antennas

To represent a basic scenario, two geographically separated transmit antennas each with line-of-sight to a receive antenna array are considered in Figure 4.5.

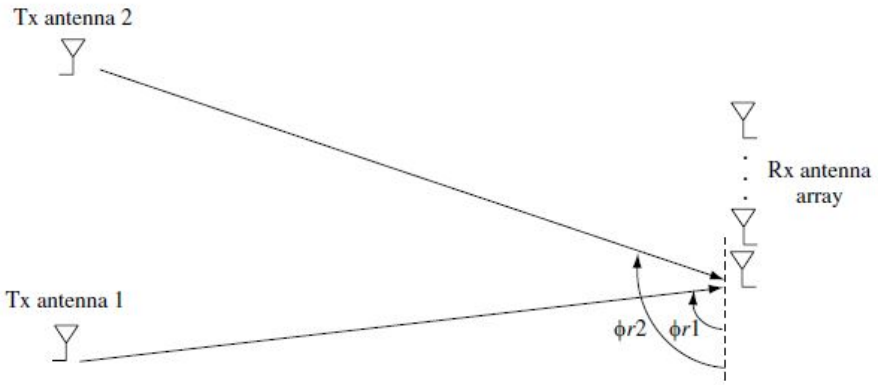

Figure 4.5: Geographically separated transmit antennas [2]

.

Since there are two a different paths for the signal, there will also be two different attenuation a and two different angle of incidences ϕ, but all considered in the vector h_k for each path 4.21

$$H_k = a_k\sqrt{n_r}exp(-\frac{j2\pi d_{1k}}{\lambda_c})e_r(\Omega_{rk}), \qquad k = 1, 2 \tag{4.21}$$

Where each vector of H_k, will be the relation of one transmitter and all the antennas of the receiver. Note that in this case we will have 2 vectors of n_r elements, so the S matrix will have also 2 vectors, giving us an extra degree of freedom.

This degrees of freedom will allow that both users can transmit and receive their data independently in the same channel and at the same frequency. This is what MIMO is designed for.

4.3.2 Angular resolvability

To end this section, a breve concepts about the resolvability in angular domain in order to see how much the antenna need to be separated to achieve the MIMO transmission.

First of all, it's important that being Ω_{r1} and Ω_{r2} directional cosines [-1,1], their difference cannot be more than 2, and at the same time, this difference cannot be 0 since it would mean that the transmitters are on the same space.

$$\Omega_r := \Omega_{r2} - \Omega_{r1} \neq 0 \tag{4.22}$$

In order to give an order-of-magnitude estimate on how large the angular separation has to be so that **H** is well-conditioned enough to use the two degrees of freedom. Knowing that the conditioning of **H** is determined by how aliened are the spatial signatures of each antenna. Being a good conditioning when

the spatial signature (4.22) is less aligned. When doing the difference of spatial signature the following computation is given:

$$f_r(\Omega_r) := \frac{1}{n_r} exp(j\pi\Delta_r\Omega_r(n_r - 1)) \frac{sin(\pi L_r\Omega_r)}{sin(\pi L_r\Omega_r/n_r)} \tag{4.23}$$

.

Where L_r is the normalised length of the receive antenna array. The angle of arrival could be extracted as[2]:

$$|cos\Theta| = \left| \frac{sin(\pi L_r\Omega_r)}{n_t sin(\pi L_r\Omega_r/n_r)} \right| \tag{4.24}$$

.

From this we can finally obtain the squared singular values of H 4.25, considering the gains in both paths are the same:

$$\lambda_1^2 = a^2 n_r(1 + |cos\Theta|), \qquad \lambda_2^2 = a^2 n_r(1 - |cos\Theta|) \tag{4.25}$$

.

Where the relation of both this values is considered the condition number of the matrix[2].

$$\frac{\lambda_1}{\lambda_2} = \sqrt{\frac{1 + |cos\Theta|}{1 - |cos\Theta|}} \tag{4.26}$$

.

We want this value to be as high as possible in order to have a well.conditioned H matrix. Meaning that $|cos\Theta| \approx 1$ is a ill-conditioned matrix and well-conditioned otherwise.

This means that the angular separation that we must have in order to have a well-conditioned H, is related with the patch antenna array dimensions.

Chapter 5

MIMO Experimental validation

Now that the radiating element of the transmission is designed. The main goal of the project can be explored. That is develop a MATLAB code that is able to simulate a MIMO transmission and finally make a real MIMO transmission in the anechoic chamber with the designed antenna and the FMCOMMS5-EBZ evaluation board extracting the main characteristics of the transmission.

5.1 MATLAB simulation

In this section the basic concepts of the MIMO transmissions explained in 4, will be used in order to make a code, able to simulate and make a representation of a MIMO transmission. The main goal of this section is being able to obtain the H matrix and represent a transmission without having to do it in real life.

5.1.1 Obtaining the matrix H

The first element we need to calculate is the relation between receivers and transmitters, the H matrix. To obtain this matrix following the equitation 4.21, the basic information needed is how the antennas are distributed in the space:

- Distance between them.
- The radiation pattern is considered omnidirectional.
- Angles they are respect to each other.
- Number of antennas.
- factor of amplitude that affects our signal during transmission. In our case this will be 1 in order to simplify the understanding.
- Frequency of the carrier: We are operating at 3.6GHz which makes our wavelength $\lambda_c = 0.083m$

In order to know how the spacing of this factors affects this H matrix and consequently the singular values matrix S, some simulations will be carried on with the code in Appendix A.2 varying the factors of distance, number of antennas and the angles:

5.1.2 1 Transmitter 1 Receiver

In this case the configuration is the following:

- 1 receiving antenna (blue).
- 1 transmitting antenna (red).
- distance= 2.6m=31.2λ
- Angle = 90° (in front)

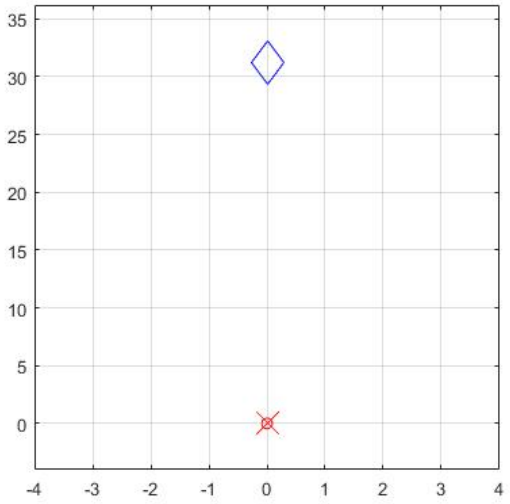

Figure 5.1: 1 receiving antenna (blue) 1 transmitting antenna (red) configuration

$$H = [0.309016994374955 - 0.951056516295151i] \tag{5.1}$$

By doing the $[U, S, V] = svd(H)$ we can obtain the three matrix that will be used in the transmission. In this case:

$$S = [1] \tag{5.2}$$

Just with the H matrix we cannot extract much information. However by doing the "svd" function in MATLAB, and extracting the singular values(5.2).

As we can see in Figure5.1 there is only one path possible, and only one relation since there is only 1 transmitter and one receiver. This will cause that the H matrix just have 1 value and consequently 1 singular value in the S matrix. This singular value means that we can not divide the channel in multiple ones. In this case, and since the amplitude voltage gain is 1, if we want to obtain the gain of the system by doing the summ of the squares of the singular values we will obtain the gain of 1

5.1.3 4 Transmitters 1 Receiver

In this case the configuration is the following:

- 1 receiving antenna seen its angular position increased 1.82° from each receiving antenna.
- 4 transmitting antenna separated 1 lambda each
- distance= 2.6m=31.2λ
- Angle = 90° (in front) of the first transmitter antenna and the receiver

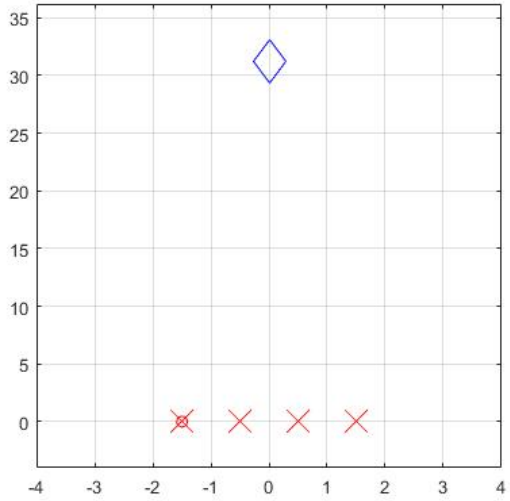

Figure 5.2: 1 receiving antenna (blue) 4 transmitting (red) antennas transmission

$$H = [0.3090 - 0.9511i \quad 0.2978 - 0.9546i \quad 0.2866 - 0.9580i \quad 0.2754 - 0.9613i] \tag{5.3}$$

$$S = [2 \quad 0 \quad 0 \quad 0] \tag{5.4}$$

As said before, the H matrix correspond to the relation between a receiver antenna and a transmitter one. This means tat if we just have 1 receiver, this matrix will become 1 vector of each relation it has with the transmitter (5.1.4). As said in the introduction of MIMO transmission, the non zero values in

the diagonal of S matrix will represent the number of independent sub-channels we are able to divide the channel. In this case, there is only one non-zero value, meaning that in this configuration we are not able to do this division and transmit more than one different signals and receive them correctly. The difference between this case and the one with just one transmitter antenna is the gain of the system. In this case doing the sum of square of the singular values with the same factor amplitude as before, we obtain a power of 4 instead of 1.

5.1.4 4 Transmitters 4 Receivers

In this case the configuration is the following:

- 4 receiving antenna separated 1 lambda each. The angular spacing each of them are being seen is increased 1.82° by each transmitter.
- 4 transmitting antenna separated 1 lambda each
- distance= 2.6m=31.2λ
- Angle = 90° (in front) of the first transmitter antenna and the receiver

It is important to note, that since in the anechoic chamber the positioner allows a circular movement, the receivers will be placed in a circular position in the simulations.

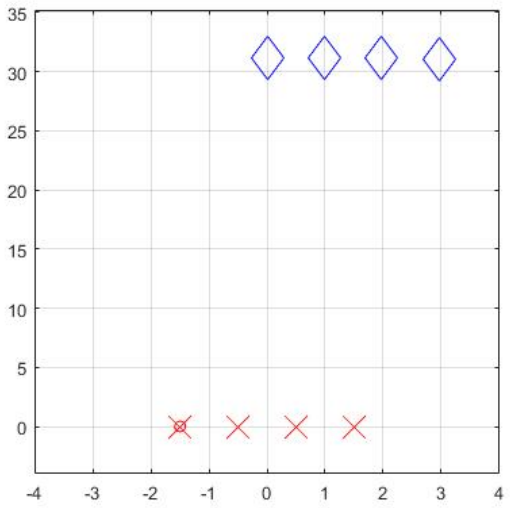

Figure 5.3: 4 receiving antennas (blue) 4 transmitting antennas (red) configuration

H=

0.3090 - 0.9511i	0.2978 - 0.9546i	0.2866 - 0.9580i	0.2754 - 0.9613i
0.3090 - 0.9511i	0.4812 - 0.8766i	0.6362 - 0.7715i	0.7687 - 0.6396i
0.3090 - 0.9511i	0.6454 - 0.7639i	0.8859 - 0.4638i	0.9954 - 0.0959i
0.3090 - 0.9511i	0.7840 - 0.6208i	0.9965 - 0.0833i	0.8767 + 0.4810i

Table 5.1: H-matrix 4Tx and 4 Rx

S=

3.8800	0	0	0
0	0.9691	0	0
0	0	0.0802	0
0	0	0	0.0024

Table 5.2: S-matrix 4tx and 4 Rx

In this case we see how the gain of the system has increased a lot (up to 16) due to the increase in the number of antennas in the receiver. In turn, we can glimpse that as there are different paths between receiving and transmitting antennas, the degrees of freedom begin to become evident. The most important in this case is that the non-zero singular values are 4, but how many of them are we able to use. In this simulation we have added no noise but in real situation this will not happen. As is seen in Table5.2, the first channel has an important gain while the other channels will have to make up for having a fewer gain.

The testing of a noise scenario will be made at the end of this section.

5.1.5 4 Transmitters 4 Receivers with distance reduced

In this case the configuration is the following:

- distance= 0.83m=10λ
- 4 receiver antenna separated 1 lambda each. Although the distance between receiver and transmitter has been reduced, the antennas have been approached in order to be seen in the same angular spacing as the previous case being 1.82°
- 4 transmitter antenna separated 1 lambda each
- Angle = 90° (in front) of the first transmitter antenna and the receiver

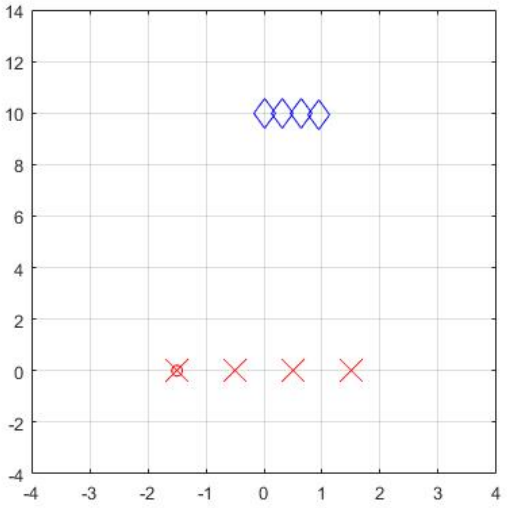

Figure 5.4: 4 receiving antennas (blue) 4 transmitting antennas (red) with 10λ distance

H=

0.3090 - 0.9511i	0.2978 - 0.9546i	0.2866 - 0.9580i	0.2754 - 0.9613i
0.3090 - 0.9511i	0.4812 - 0.8766i	0.6362 - 0.7715i	0.7687 - 0.6396i
0.3090 - 0.9511i	0.6454 - 0.7639i	0.8859 - 0.4638i	0.9954 - 0.0959i
0.3090 - 0.9511i	0.7840 - 0.6208i	0.9965 - 0.0833i	0.8767 + 0.4810i

Table 5.3: H-matrix 4Tx and 4 Rx with different distance

S=

3.8800	0	0	0
0	0.9691	0	0
0	0	0.0802	0
0	0	0	0.0024

Table 5.4: S matrix 4tx and 4 Rx with different distance

In his case it is seen that what increases the value of the singular values is not the distance between antennas. As is seen in Table 5.4, the singular values are exactly the same as the previous case seen in Table 5.2.

5.1.6 4 Transmitters 4 Receivers with angular distance increased

In this case the configuration is the following:

- distance= 0.83m=10λ
- 4 receiving antenna separated 1 lambda each. The angular spacing each of them are being seen is increased 5° by each transmitter.
- 4 transmitting antenna separated 1 lambda each.
- distance= 0.83m=10λ
- Angle = 90° (in front) of the first transmitter antenna and the receiver

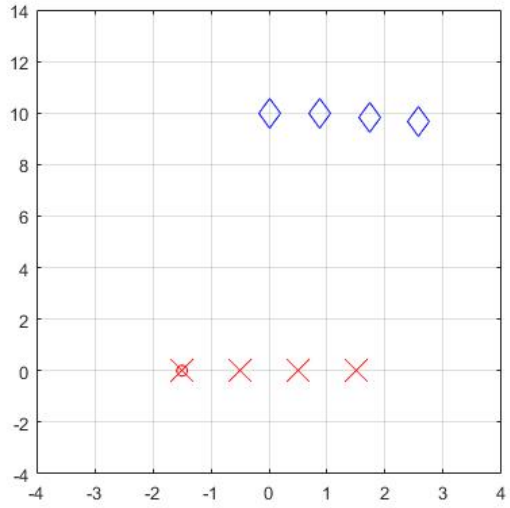

Figure 5.5: 4 receiving antennas (red) 4 transmitting antennas (blue) 5º of angular spacing

H=

1.0000 - 0.0000i	1.0000 - 0.0022i	1.0000 - 0.0044i	1.0000 - 0.0065i
1.0000 - 0.0000i	0.8549 + 0.5188i	0.4654 + 0.8851i	-0.0488 + 0.9988i
1.0000 - 0.0000i	0.4598 + 0.8880i	-0.5704 + 0.8214i	-0.9946 - 0.1041i
1.0000 - 0.0000i	-0.0698 + 0.9976i	-0.9919 - 0.1269i	0.1590 - 0.9873i

Table 5.5: H matrix 4tx and 4 Rx with different angular difference

S=

3.2819	0	0	0
0	2.2025	0	0
0	0	0.6124	0
0	0	0	0.0537

Table 5.6: S matrix 4Tx and 4 Rx with different angular difference

The final scenario simulated shows us that one of the main factors that influences the value of the singular values seen in Table 5.6 is the angle difference each antenna has with the respective transmitter or receiver array. In this case the value chosen has been 5° (an increase of spacing) to see if it influences positively or negatively. As seen in 5.6 the value of the total gain is the same (16), but the distribution of the power along the sub-channels is more equal. This means that the more separated are the antennas (spatial signature), the better distributed is the gain among the sub-channels. In this case we see how two of the sub-channels could be used in order to increase the capacity and the other 2 sub-channels with less gain may not be used due to the noise.

5.1.7 QPSK transmission

To end this section, the validation that the H matrix obtained together with the procedure explained in Chapter4, allow us to realise a MIMO transmission and receive the data will be carried out. The main goal is that if we apply (4.10), the result is the same as the transmitted signal.

To do so, the idea is to represent the scenario 5.1.4, this means that we will have 4 transmitters, 4 receivers. As seen before, this case allows to do a 4 signal transmission in the same channel (sub-divided in 4). However to make this scenario more real, some noise will be added in order to see how it influences the receiving part of the system.

The signal chosen to transmit is a QPSK symbol transmission. Remember that a QPSK transmission is formed by 4 different symbols (Figure 5.6):

$$QPSK_{symbols} = \pm\sqrt{2}/2, \pm\sqrt{2}/2i \tag{5.5}$$

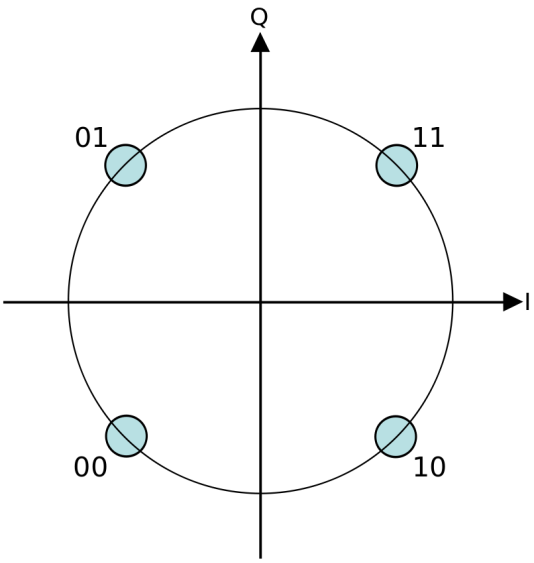

Figure 5.6: QPSK symbols

All the following code can be seen in AppendixA.3. We will send a random stream of these values distributed between the 4 transmitting antennas, spacing it with the 4 channels. Leaving the 2 first symbols as a 0 in order to have a reference at the receiver. The idea is to transmit a random stream of 4096 QPSK symbols for the channel, divided in 4 different sub-channels.

If we follow the patch seen in figure 4.2, the operation needed are the follwing;

$$Y = pinv(S)U'U(W + SV'VX_f.') \tag{5.6}$$

$$Y = pinv(S)U'(Wu + USV'VX_f.') \tag{5.7}$$

$$Y = pinv(S)U'(Wu + HVX_f.') \tag{5.8}$$

Where:

- Y: It is the stream that is recovered
- X_f: Data stream transmitted
- H: Channel matrix (obtained in the previous section 5.1.4)
- S: Parameters of the degrees of freedom extracted from H
- U: rotation matrix of post processing signal. Extracted from H with the svd function.
- V: rotation matrix of pre processing signal. Extracted from H with the svd function.
- W_u: Transmission noise added in the H matrix

The code to obtain all this function data is seen in Apendix A.3.

Remember that in this case the, scale factor that was considered for the H matrix calculation was 1 (0dB). In our case we tried different values at the noise power to see which was the final signal received.

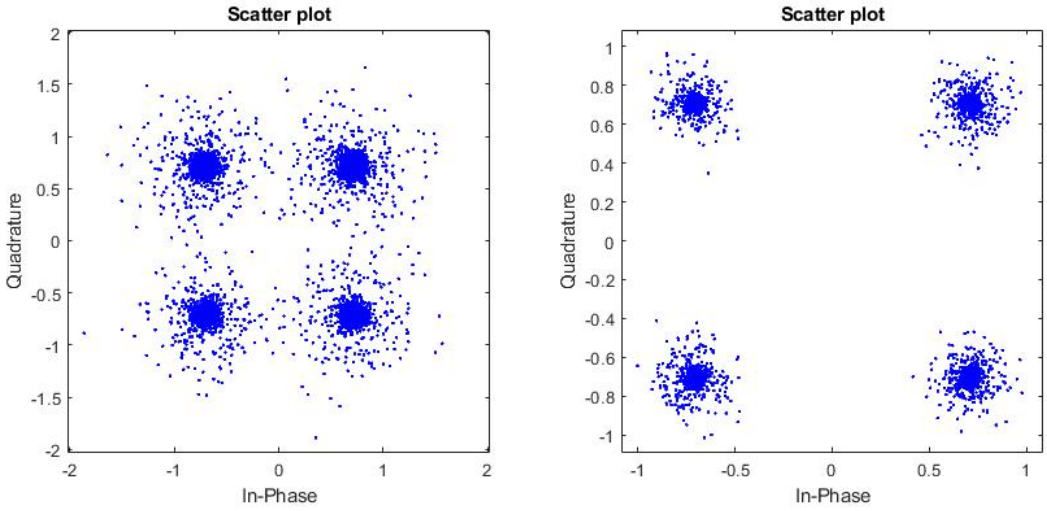

(a) -10dBW (b) -20dBW

Figure 5.7: Noise power

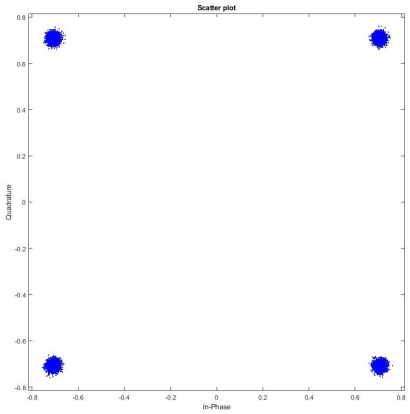

Figure 5.8: Noise power -40dBW

As is obvious to think the less noise power, the less influence on the signal it will have. This means that in this case where the the signal power is 0dB and the noise power is established, at -10dBW the 4 symbols started to get mixed and in some cases there will be errors at the receiver.

5.2 Anechoic chamber measurements

Until now, only simulations have been done. This means that no real data has been transmitted. In this section the main goal will be to carry out a MIMO transmission with the antenna fabricated in 3.

5.2.1 Configuration of the measurement

In order to make the 4 channel transmission, the FMCOMMS5-EBZ evaluation board [16] is needed. This board allows us to modify the radio frequency at which it works, in order to fulfill the application needs. This change of frequency is quick and via software in the 70 MHz - 6 GHz range. Within this range we can have a channel bandwidth of 200 kHz - 56 MHz. In addition, contains 4 transmitters and 4 receivers, which would allow us for a 4x4 MIMO test. Although in this case only a 4x1 will be needed, meaning that only 1 receiver will be connected to the board. This transmitters an receivers are part of two AD9361 chips that have 2 transmitters and 2 receivers each (Figure 5.9)

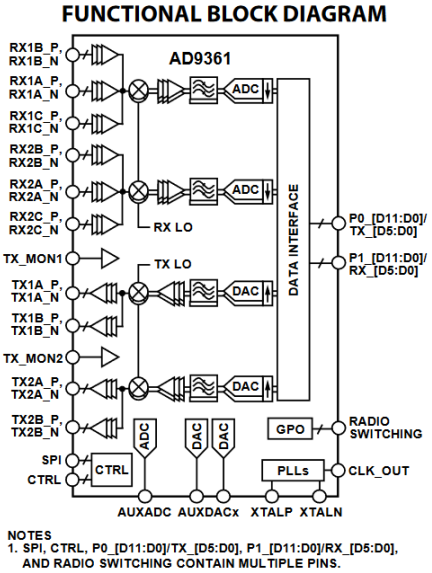

Figure 5.9: AD9361[3] chip scheme

This board will act as FPGA (Field Programmable Gate Array) and provide an interface for the AD9361 chips that it uses to connect to a computer and be programmable. Besides it also provides synchronisation between these chips so that they can be used in MIMO transmissions, which is our case. In order to communicate with a computer, another board is needed. The Zynq ZC706[27] will provide the memory, the feeding and different ports in order to connect the principal board to the computer and the oscilloscope to make the measurements. See in 5.10 how the two boards are connected and which will be the different peripherals used.

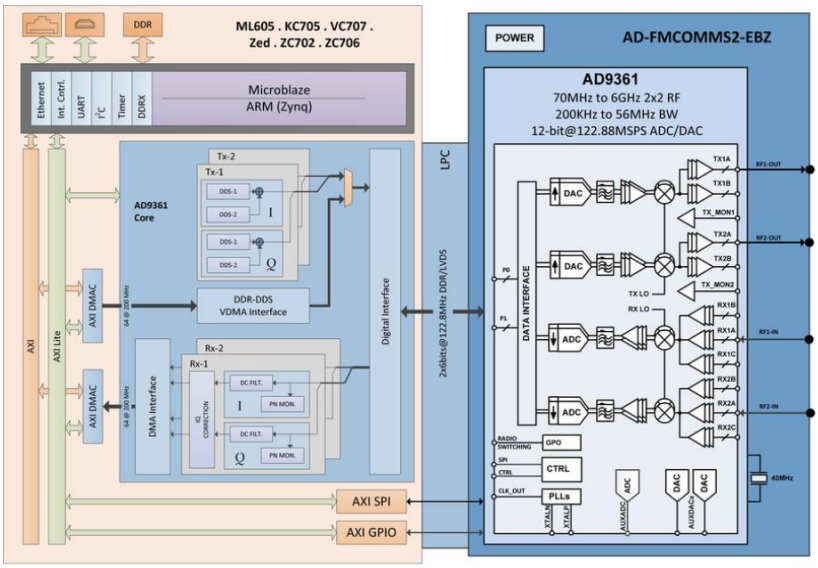

Figure 5.10: FMCOMMS5-EBZ connection with Zynq-ZC706

In regard of the anechoic chamber, will have the cylindrical probe antenna as a static receiver seen in Figure 5.13a. Separated a distance of 2.6 meters, there will be our array of 4 patch antennas Figure 5.13b connected behind to the 2 boards explained previously. Obviously, the receiver must be also connected to the board. This means that a wire must cross the inside of the anechoic chamber. We will have to be careful with the transmitter movement in order not to tangle the wire with the absorption cones.

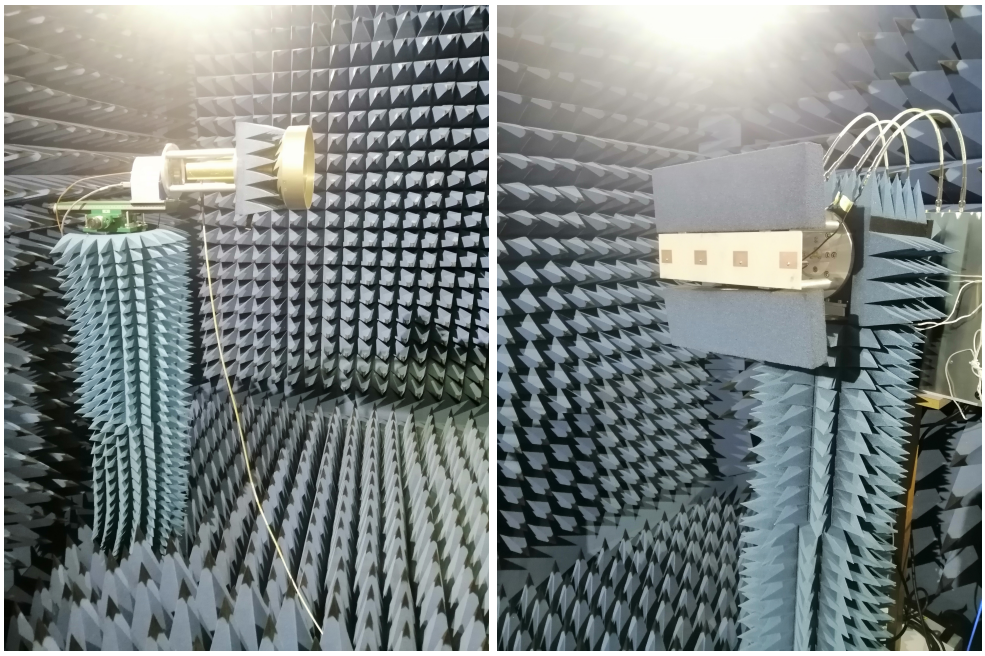

(a) Receiver antenna (b) Transmitter antenna

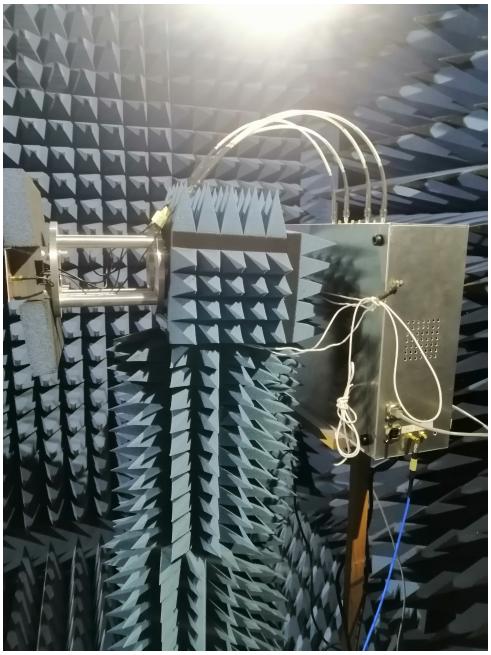

(c) Connections of the Tx antenna

(d) FMCOMMS5-EBZ and Zynq-ZC706 boards

It is important to note that the values received by the receiver antenna from the 4 different transmitter are the values of the H matrix, since they represent the channel gain when transmits antenna i and receives antenna k.

We want to represent a 4x4 MIMO transmission, but only 4 transmitters antennas and 1 receiver which is static. The solution to this is make the transmission with the 4 antennas and the receiver. Collect all the data received in order to calculate the H matrix or analyse the received data. Then change the angle of the transmitter to represent that the receiver is located in another position and seem it is different from the previous one.

In conclusion, the procedure will transmit the stream in one position, collect all the data and then change the angle of the transmitter. Once it is changed transmit again and collect the data. This procedure will be done for as many receivers we want to calculate. In our case there will be 4 receivers, so 4 different transmission with 4 different angles. When all the transmissions are done we will be able to calculate the H matrix by combining and processing the values received, at the same time apply the pos/pre processing transformations neeeded for the MIMO transmission.

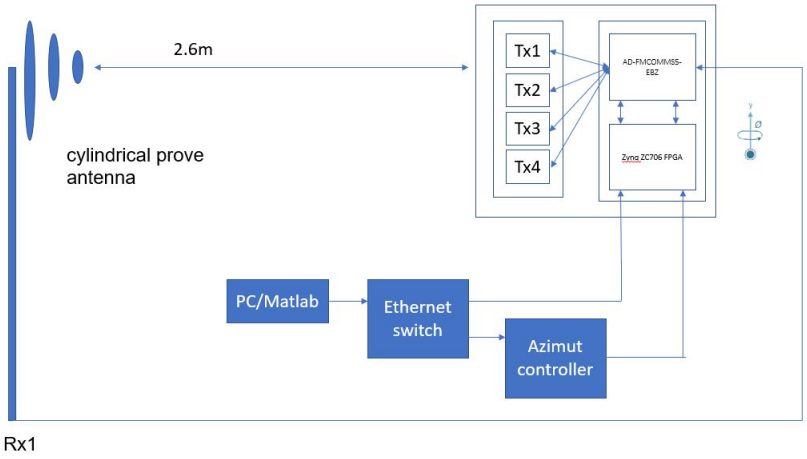

Figure 5.11: Configuration of the anechoic chamber

To end the configuration we need to program the FMCOMMS5-EBZ evaluation board. To do so the board have an specific program for itself or to do it faster installing some MATLAB libraries from Analog devices that allow us complete communication between MATLAB and the board. This will also facilitate the pos/pre processing code, since they will be programmed in MATLAB too.

This libraries allow the use of Simulink that recreates the input and output signals of the board. At the same time, change the values for the transmission. In our case the final configuration 5.12 will be:

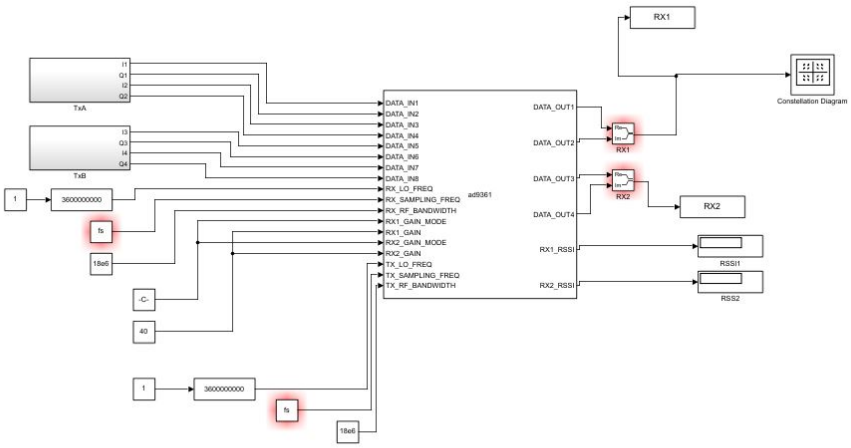

Figure 5.12: Final simulink configuration

- Operating frequency: 3.6 GHz
- Sampling frequency: 30.72 MHz

- Bandwidth: 18 MHz
- Gain: 40 dB
- Each input and output is formed by 2 variables the quadrature and phase with the same name as the QPSK signal determined before in matlab code.

5.2.2 Measurement procedure

Below is a brief description of the steps to follow the measures and the results obtained:

1. First of all, in order to make a MIMO transmission, we need to get the array of channel H. This array allows us to do both preprocessing and postprocessing of the signal to get the measurements right.

   To perform this measurement, we will use the code calMIMO that can be found in Appendix A.4. This code consists of first of all define how the transmitted data will be. In our case a QPSK of 1024 symbols, where each symbol will consist of 10 samples. 15 frames will also be sent. Once we have the 8 (phase and quadrature of the 4 transmitting antennas) initialised channels (with 0), and we have calculated each time a sample is taken (1 / sampling frequency), we will start with one transmission. Because we only have one receiving antenna, we can only measure the signal received by one receiver from each of the transmissions. This means that we only get one row of the matrix H for each transmission we make. Because of this, we will have to transmit 4 times in order to obtain the complete H matrix.

   It should be noted that due to the FMCOMMS5-EBZ board itself and the AD9361 chips, the measurements suffer from not transmitting exactly the symbol stream in the order that was programmed. This fact will make us programm a MATLAB function "calconvframe" seen in Appendix A.5 that align the transmission streams so we can compare them correctly.

   It does this thanks that in the initialisation of the stream is composed of 0 and when doing the convolution, it is possible to adjust until all 4 streams have the 0 at the beginning.

2. In the code (calMIMO), what is done in each transmission is to create a random QPSK signal, for only 1 of the channels, transmitting it and by doing the stream alignment correction. Its signal tension is also calculated in the receiving antenna. This tension becomes the conjugate average, which would be equivalent to the value of S-parameter. This process is performed for each transmitter channel, until we have the row of the complete matrix H. The next step is to change the angle position of the antenna transmitter / receiver the only one that can move in our case is the transmitter, so it represents as if we had another receiving antenna in that position. If the application has 4 receiving antennas, this process has to be repeated 4 times in order of having a 4x4 H matrix.

3. Once we have the calculated H matrix, all we have to do is its svd decomposition in order to obtain the values of V, U and S. With this values all the post/pre processed can be done, together with another transmission set. This process will be done in the code "Executioncode" that can be found in Appendix A.6.

Remember that, each transmission is equivalent as one receiver, so the code will be executed 4 times. Each time with a different angular position of the transmitter.

4. Once we have the 4 transmissions made and put together in one matrix, all we need to do is do it post processed signal, multiplying by the inverse of the matrix S and the conjugate of the matrix U.

5.2.3 10° of angular spacing

As seen in subsection5.1.6, when the antennas are more geographically separated, the more equally distributed are the gains through the sub-channels. Having this in mind, the idea of the first measurement is to have the best results possibles by separating the antennas 10°.

The final configuration of the system is the following:

- 4 receivers (4 measurements)
- 4 transmitting antenna separated 1 lambda each. The angular spacing each of them are being seen is increased 10° by each transmitter.
- distance between transmitter-receiver=31.2λ

Once done the first step (H matrix obtaining), we see the following result:

H=

-30.0666 -83.6522i	-76.6968 -72.9713i	45.4416 -89.5895i	68.7764 -55.9467i
-78.4105 +15.4643i	-94.9543 -24.7179i	75.3762 -48.3131i	49.6193 +64.2344i
18.0643 +66.3337i	-85.3795 +27.6475i	79.4796 + 1.0780i	-58.2480 +39.7536i
60.6714 -13.1127i	-59.7972 +47.9508i	60.2023 +40.8198i	-36.6696 -50.7203i

Table 5.7: H matrix 4tx and 4 Rx in anechoic chamber with 10° angle spacing

That by itself tells us nothing, but that if we do its decomposition, its matrix S should give us an information similar to the one we had simulated previously:

S=

230.3318	0	0	0
0	191.3054	0	0
0	0	139.3674	0
0	0	0	40.1581

Table 5.8: S matrix 4Tx and 4 Rx in anechoic chamber with 10° angle spacing

S=

2.4890	0	0	0
0	2.4115	0	0
0	0	1.9290	0
0	0	0	0.5181

Table 5.9: S matrix 4Tx and 4 Rx simulation with 10° angle spacing

In the following matrix 5.8, we can see which are the singular values of the simulated system as measured in the anechoic chamber. While the results seem drastically different, we have to consider that we have introduced system power: whether amplifiers at 40dB, antenna gain or camera noise, space losses, which will cause the value to change. However, if we want to know if the results are related to each other, we could make their relationship (5.9). The matrix simulated will be with the same values as the measurement. This gives an S matrix 5.9. And we see clearly how the relationship in Table 5.10 is very similar for all channels. The small differences that can be seen may be due to small changes in wiring or when introducing the power of the system (amplifiers, noise antennas ...) to the measurement.

$$Relation = S_{measured} S^*_{simulated} \tag{5.9}$$

Relation=

0.0108	0	0	0
0	0.0126	0	0
0	0	0.0138	0
0	0	0	0.0129

Table 5.10: Relation measurement vs simulation

Once we have the channel matrix, all that remains is to do the pre processing on the signal we want to transmit for the 4 antennas (1024-symbol QPSK), and send it over the channel. This last step is to send it through the channel will perform 4 times, in order to simulate the 4 receiving antennas with an angular spacing of 10°.

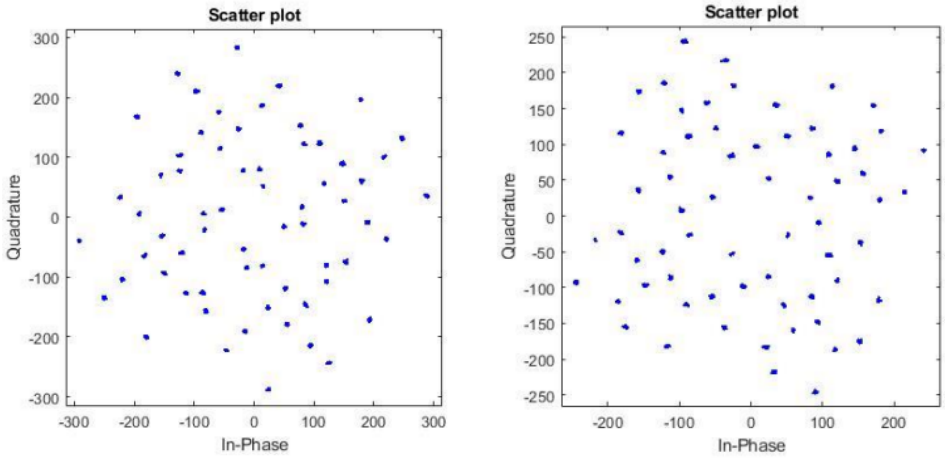

(a) 1st Receiver antenna (b) 2nd receiver antenna

Figure 5.13: Signal at the receivers

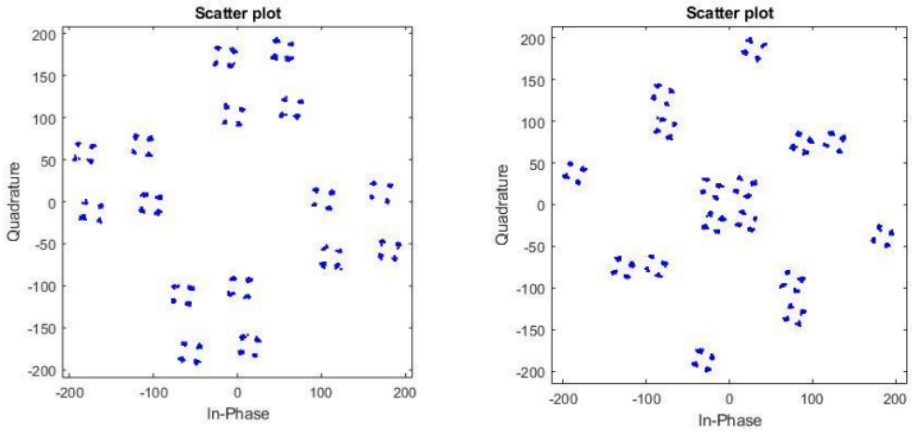

(a) 3rd receiver antenna (b) 4th receiver antenna

Figure 5.14: Signal at the receivers

Figures 5.13 and 5.14 show signals at the receivers. As such, these results do not make much sense, as we have applied a pre processing to the signal sent, but not post processed, so this will be our next step.

Once we have made the transmission for the 4 receivers, we group everything in a matrix and do the post processed, obtaining the following result:

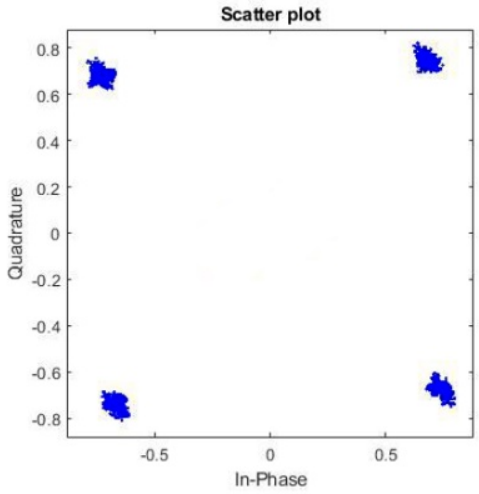

Figure 5.15: Final signal received

In this case we can already clearly see how we were able to recover the signal sent, along with the reference 0s used to align the streams. This means that we can perfectly recover the signal sent by the 4 channels, using the MIMO application in this scenario. The noise introduced in this configuration will be analysed in section 5.3.

5.2.4 1.82° of angular spacing

To make a measurement where the final reception could be affected by the noise. To the point where one receiver would not be able to differentiate the symbol. The angular spacing thought, is the one given if the same array was situated in the receiver at the distance of 31.2λ. In this case this angle would be 1.82°.

The final configuration of the system is the following:

- 4 receivers (4 measurements)
- 4 transmitting antenna separated 1 lambda each. The angular spacing each of them are being seen is increased 1.82° by each transmitter.
- Distance between transmitter-receiver=31.2λ

Once done the first step (H matrix obtaining), we see the following result:

H=

-30.0666 -83.6522i	-76.6968 -72.9713i	45.4416 -89.5895i	68.7764 -55.9467i
-49.6859 -70.5098i	-81.7420 -57.4798i	49.2743 -86.5199i	77.6333 -39.4556i
-67.0694 -54.9455i	-87.7468 -50.1055i	54.0816 -80.0188i	85.0066 -13.4524i
-77.2892 -34.7056i	-91.0203 -40.2423i	62.7860 -73.7321i	83.7103 +10.5865i

Table 5.11: H matrix 4Tx and 4 Rx in anechoic chamber with 1.82° angle spacing

That by itself tells us nothing, but that if we do its decomposition, its matrix S should give us a relation. similar to the one we had simulated:

S=

365.7709	0	0	0
0	78.6351	0	0
0	0	6.8307	0
0	0	0	2.7859

Table 5.12: S matrix 4tx and 4 Rx in anechoic chamber with 10° angle spacing

Clearly, in this case we see the gain of the different channels has a much more large relation than the previous case. This can make it much more difficult to recover the signal transmitted by the weaker channels.

Once the post process signal is done, the final result is seen in Figure 5.16

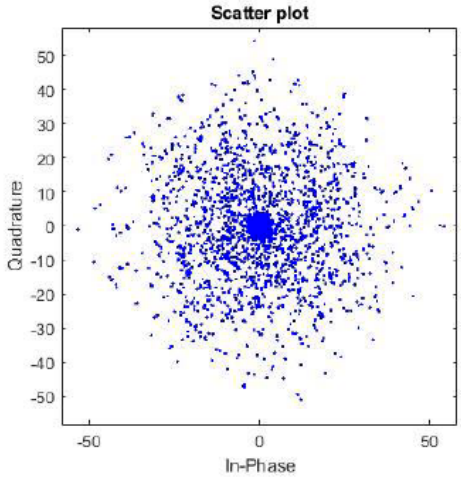

Figure 5.16: Final signal received

Clearly, we cannot say that we are recovering the transmitted signal, as we cannot differentiate any

QPSK symbol, but if we focus more on the centre of the Figure 5.16 we will see how at least one of the channels is receiving what it should be (Figure5.17).

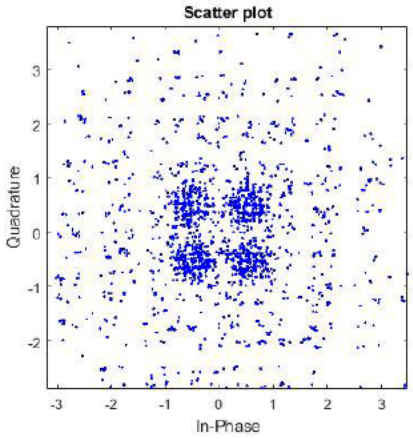

Figure 5.17: Final signal received

5.3 Noise

In order to properly analyse the noise we have in the measurements received. The noise received by each of the four symbols of the reception (will be made by the 4 channels of transmission and by the 4 angles representing the 4 reception channels). To make the measurements more visual, we have chosen the channel where the angular spacing is 10^{o}, since this case allows us to see more clearly what we should have in each channel. There will be 2 tables that will compare the signal to noise ratio for each sample analysed, and also, another table comparing the correction error that occurred in each of these samples. To obtain the corresponding data, we took advantage of the system calibration code (calcconvframe) to stop streaming just when only 1 channel was broadcast, save the data transmitted and received, and do the same for the other 3 channels. This process will be repeated on with the other 3 angles (16 samples).

Only one Figure5.18a will be displayed with the noise power of each channel, as they are all very similar, there is no need to repeat the same image. The same for the symbols received by each receiver for each transmitter in Figure 5.18b.

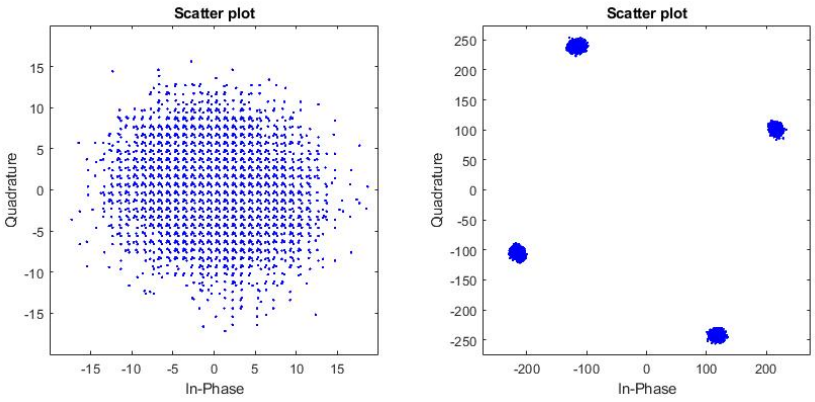

(a) Noise at 1st receiver vs 1st transmitter (b) Symbols received

Figure 5.18: Noise and reception of the first transmission

In Figure 5.18a is the representation of the noise received by the first antenna in the transmission of the 1st transmitter. It also can be seen that the noise seems to be quantified since it has determined values. When all the noise measurements are done, it looks like all the noise for each channel has similar values, so only one Figure 5.18a will be shown.

Although the noise is similar in all the channels, since the post processed signal will introduce an amplitude factor on the received signal, the noise will be amplified in these different factors. This will make that some channels can not be used.

From , the representation of the mean symbol will be made, in order to obtain the error at the reception. A comparison between the different symbols will also be made to know if the error is equal in each symbol or not. Here the idea is to find if the error is a not perfect accuracy of the transmitter, or if its an error of the configuration that can be corrected in the post processing part.

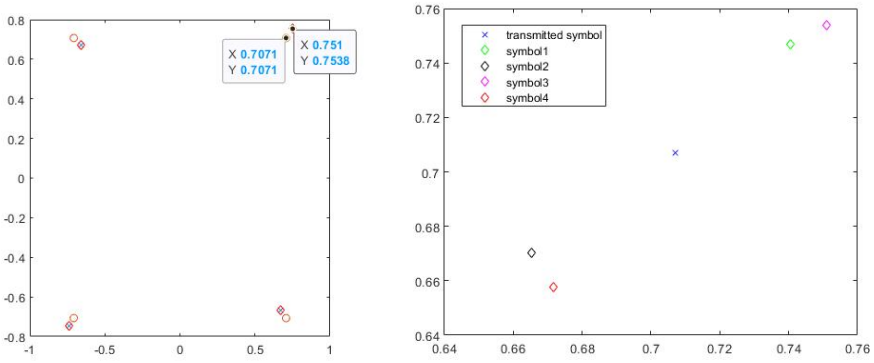

(a) 1st receiver vs 1s transmitter (b) Error of the symbol

Figure 5.19: Error at the 1st receiver for the 1st channel

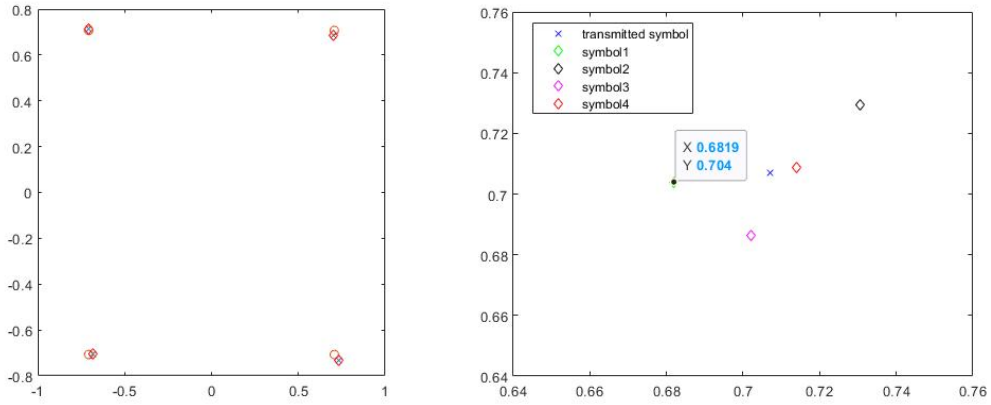

(a) 2nd receiver vs 2nd transmitter

(b) Error of the symbol

Figure 5.20: Error at the 2nd receiver for the 2nd channel

The signal transmitted will be in circles, and will be considered as the perfect values for a QPSK transmission. The diamonds will be the value of the received signal. In order to fin the error of the transmission we have to compare the transmitted symbol and the received symbols to see how the constellation changes.

What we see in the following images is what we will get in most of the following samples, and it is as follows:

- In Figure 5.19a and 5.20a we see how the received symbols have not the exact same value as the transmitted ones, and this happens in each transmission.
- On the other hand, in Figures 5.19b and 5.20b, we see how each symbol has a different error compared to the exact value of the constellation in each transmission. This means that the error is not the same for each symbol

.

In this section what can be seen is that the FMCOMMS5-EBZ board has an intrinsic error that depends on the transmitted symbol (it can not represent exactly the QPSK values). This will cause that when calculating the channel matrix H, the estimation will not be made perfectly. At the same time, this error will appear as a non-Gaussian noise that can not be corrected.

The summary of each symbol error for each transmission will be seen in the following Tables:

Signal Power(dB)

Receiver	1				2			
Channel	1	2	3	4	1	2	3	4
Average	48,07	50,01	49,69	48,79	47,64	49,32	48,60	47,89
Symbol 1	48,52	50,08	49,76	48,89	47,45	49,15	48,44	48,07
Symbol 2	47,58	49,91	49,60	48,66	47,93	49,61	48,86	47,83
Symbol 3	48,62	50,20	49,86	49,00	47,47	49,17	48,46	47,87
Symbol 4	47,54	49,89	49,57	48,93	47,72	49,38	48,64	47,86

Table 5.13: Signal power receivers 1 and 2

Signal Power(dB)

Receiver	3				4			
Channel	1	2	3	4	1	2	3	4
Average	46,88	49,06	47,95	46,96	46,11	48,02	45,94	46,11
Symbol 1	46,81	49,00	47,92	46,91	46,28	48,37	46,11	45,93
Symbol 2	46,83	48,99	47,87	46,88	45,97	47,69	45,80	46,22
Symbol 3	46,96	49,17	48,04	47,07	46,14	48,25	45,98	46,17
Symbol 4	46,94	49,11	48,00	47,01	46,06	48,25	45,88	46,14

Table 5.14: Signal power receivers 3 and 4

Noise power(dB)

Receiver	1				2			
Channel	1	2	3	4	1	2	3	4
Average	16,43	16,51	16,53	16,40	16,01	16,61	20,99	19,76
Symbol 1	16,84	16,69	16,63	15,97	16,10	16,54	25,32	16,77
Symbol 2	16,29	17,02	16,26	16,91	16,11	16,92	16,72	22,73
Symbol 3	16,59	16,19	16,11	15,98	15,60	16,31	25,41	16,81
Symbol 4	16,02	16,14	17,12	16,75	16,22	16,66	16,52	22,74

Table 5.15: Noise power receivers 1 and 2

Noise power(dB)

Receiver	3				4			
Channel	1	2	3	4	1	2	3	4
Average	16,04	16,47	15,88	16,12	16,25	17,29	15,66	16,32
Symbol 1	16,15	16,14	15,99	15,04	15,45	17,43	16,05	16,84
Symbol 2	15,42	16,76	16,32	16,63	16,56	16,93	14,67	15,27
Symbol 3	16,44	16,10	15,40	16,34	16,23	17,12	16,25	17,03
Symbol 4	16,15	16,86	15,80	16,46	16,75	17,70	15,66	16,14

Table 5.16: Noise power receivers 3 and 4

In terms of received power and noise power, we can see that in general terms, for each angle the received signal power decreases (49.4dB, 48.36dB, 47.7dB, 46.5dB average), about 0.7-0.8dB for every 10^{o}. If we look at the radiation pattern of the array this decrease in the signal power has a lot of sense, since the patterns are not omnidirectionals. While the received noise power is quite similar at all angles, the measurements of the symbols 1 and 3 for channel 3 of the 2nd receiver and symbols 2 and 4 of channel 4 for the second receiver, the noise power is much higher than the other measures taken.

Below is the table where all the relative errors of each symbol have been noted with respect to the perfect value of the constellation QPSK $\pm$ 0.707 $\pm$ 0.707i:

Relative error %

Receiver	0				1			
Channel	1	2	3	4	1	2	3	4
Symbol								
1	5,184	0,769	0,746	1,130	2,587	2,537	2,386	1,041
2	5,575	1,411	1,298	1,715	3,354	3,255	3,091	2,084
3	6,407	2,064	1,909	2,354	2,336	2,150	2,099	1,875
4	6,082	1,687	1,661	1,992	0,880	0,692	0,608	0,668

Table 5.17: Relative error of the symbols in receiver 1 and 2

Relative error%

Receiver	3				4			
Channel	1	2	3	4	1	2	3	4
Symbol								
1	0,960	1,012	0,663	0,913	1,988	4,077	2,031	2,128
2	0,882	1,304	1,176	1,243	1,784	3,847	1,818	1,889
3	1,257	1,359	1,333	1,447	0,560	2,662	0,601	0,821
4	1,335	1,108	1,037	1,078	0,983	2,976	1,020	1,300

Table 5.18: Relative error of the symbols in receiver 3 and 4

As can be seen, the error in this case does not cause the signal to ever cross another quadrant. Therefore, we could recover the symbol perfectly. As we have seen in the pictures, the error in each symbol is different, causing that we can not correct the symbols with the same values for all. We see that it does not follow any pattern error either, which makes us think that the error is very much related to the fact that we are not transmitting exactly the QPSK symbol $\pm$ 0.707 $\pm$ 0.707. This fact will cause that the H estimation is not perfectly accurate to the real scenario.

We take the measurements again and save them with the 10° angle spacing scenario to check that the results are similar to the previous one.

The measurements are similar in all aspects, both signal strength and noise power. And as for the error in the final symbol received, although the results are not the same, we could consider that these variations are due to the simple fact of re-measuring as they are very similar.

It is important to note that in this measurement, the noise values that were high in the previous measurement, have the same value as the rest. This could mean that the slightly higher noise measured was just an error from the receiver or from the transmission, that can happen.

In this case measured power difference varies between -0.55dB and 1.77dB in the worst case. Therefore, we will consider that the measurement corresponds to the expected and will be used to extract results close to the calculation of the matrix H.

These variations may be due to:

- The simple act of re-measuring the transmitted signal
- The system is influenced by not being exactly dependent on whether the door of the room is more open or more closed.
- The amplifier may not amplifying perfectly steadily at 40dB.

In the noise power comparison, we see a case very similar to the signal power. The measurements are quite similar around 16-17dB, but with some differences. Therefore we will consider that the gains and noise used in the H matrix estimation are consistent and fit for the measurement. We also see how in the

first case the noise turned out to be higher in the symbols 2 and 4 of channel 2 by the receiver at 30^{o} (4th receiver). However, the noise power values that were high in the first measurement seen in Table 5.16, were not in this case. This makes us think that maybe the 2nd AD9361 chip in the FMCOMMS5-EBZ may have some calibration problem, although it is not repeating every transmission.

Finally we have the comparison of the relative error between the transmitted symbols and the received symbols. We conclude that there is a relative error between 0.7% and 3% compared to the symbol of the constellation QPSK. However, in this case this error will not prevent to loose any channel

5.4 Scenario limitations

To end this project, the main goal is to find the limits of our scenario in the anechoic chamber. With the H and S matrix obtained from the 1st measurement we can obtain the amplitude factor relation between the simulation were, it was considered 1 and the real factor. In this case the relation obtained comparing the S matrix in both cases was 250 (24dB) 5.9 and 5.19. Knowing that the noise power is about 16.5dB we can now make the exact simulation in order to obtain a real value.

S=

694.2072	0	0	0
0	600.5953	0	0
0	0	437.9085	0
0	0	0	127.8573

Table 5.19: S matrix measured at the anechoic chamber

To prove that the simulation is similar to the real scenario, a comparison between the final received signal between them:

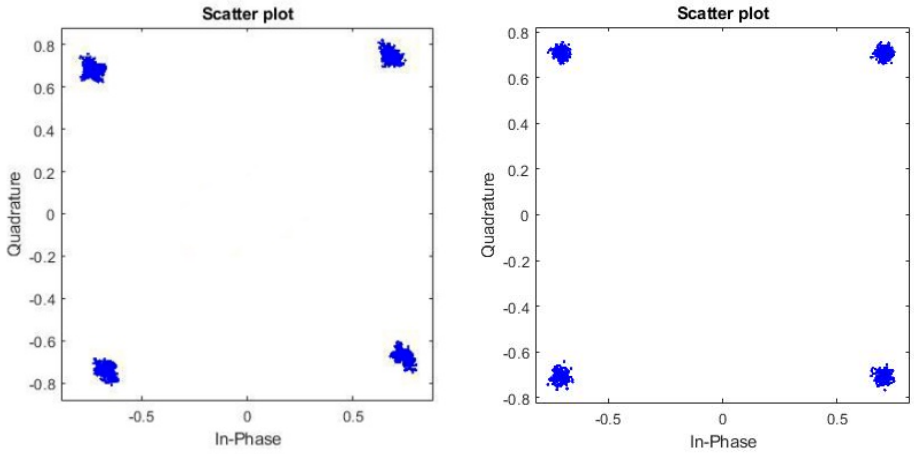

(a) Real scenario reception

(b) Simulation scenario reception

Figure 5.21: Measurement vs simulation

As we can see in Figure 5.21, the reception in the simulation is the same as the measurement, proving that the simulation corresponds to the real scenario and can be used to find its limits without carrying out a real transmission.

As we have seen before, the difference between the actual measurement and the simulated measurement, it was basically a multiplicative factor related to the power of the whole system. In our case, this factor is about 250-230, which is what we need multiply our matrix H so that it takes into account the gain of the system. If we didn't do this and only add the 16.5dB of noise, we wouldn't be considering all the system gain factors and considering that we had set it as 1, it would seem that we would have a lot more noise than we actually should.

As seen before, with antennas separated 10°, all the channels are available. This means that all transmissions can be received with no errors. But, now that we have the simulation calibrated as the real scenario we will find at which antenna's angle spacing this channels starts fading.

The loss of the fourth channel, starts at a spacing of 4°, although the channel starts degrading at around 4°, but not enough to loose the data for the noise interference.

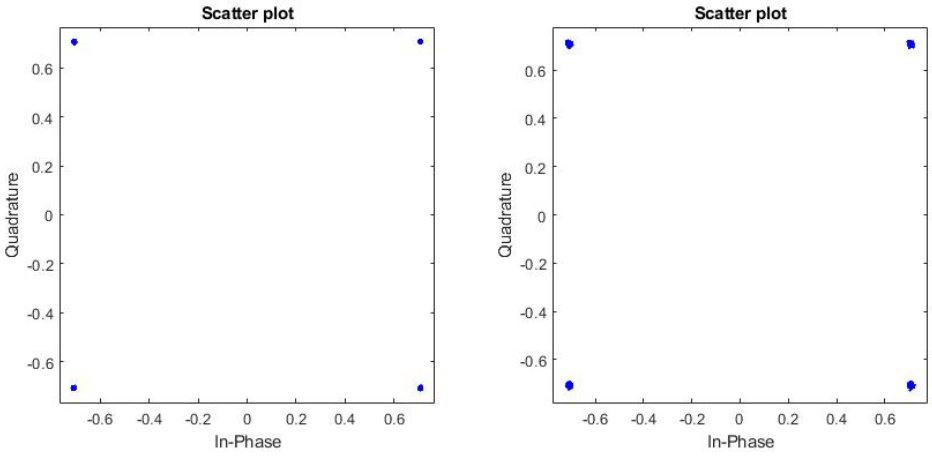

(a) 1st channel reception (b) 2nd channel reception

Figure 5.22: Channel 1 and 2 reception with an antenna's angular spacing of 4°

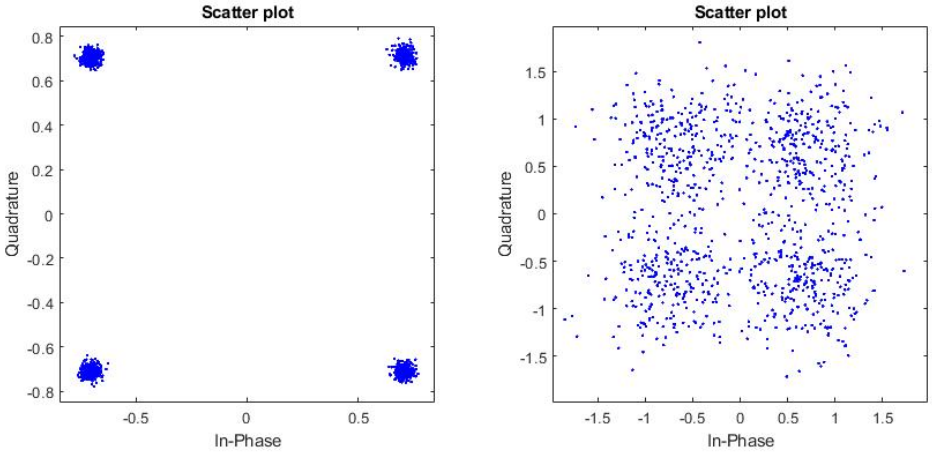

(a) 3rd channel reception (b) 4th channel reception

Figure 5.23: Channel 3 and 4 reception with an antenna's angular spacing of 4°

As we can see in Figures 5.22 and 5.23, all the channels have a well received QPSK constellation but the 4th channel (Figure 5.23b). However in this 4th channel a large percentage of symbols continue within the corresponding quadrant. This mean that not all the symbols will be well received and an error will be made. In this situation, it depends on the application used if this error is negligible or not.

In order to find the SNR where the channel is not able to receive all the symbols correctly. A comparison between the signal power received and the noise power of 16.5dBW will be done(Table 5.20).

		Receiver			
		1	2	3	4
CHANNEL	1	64,8	59,6	45,9	23,4
	2	64,8	59,6	45,9	23,4
	3	64,8	59,6	45,9	23,4
	4	64,8	59,6	45,9	23,4

Table 5.20: Signal power for each receiver with an angkle spacing of 4°

We can now tell that if the noise power is 16.5dBW and the power of the 4th channel is 23.4dB. With an SNR of 6.9dB, that for a QPSK is a bit error rate of 0.01 [28], the channel can be discarded.

Continuing with the limits of the scenario, the loss of the 3rd channel in this scenario comes with an antenna angular spacing of 1°. Where the symbols received in each channel are seen in Figure 5.28

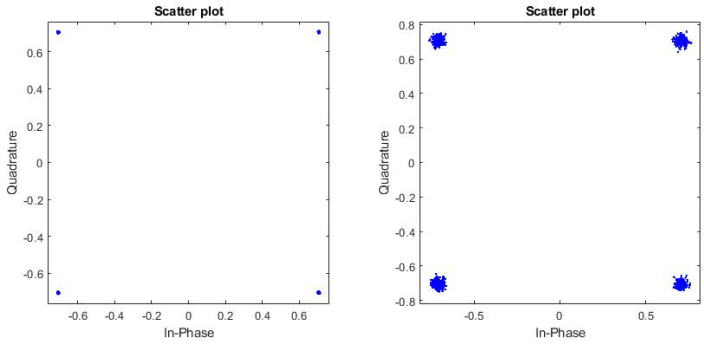

(a) 1st channel reception (b) 2nd channel reception

Figure 5.24: Channel 1 and 2 reception with an antenna's angular spacing of 1°

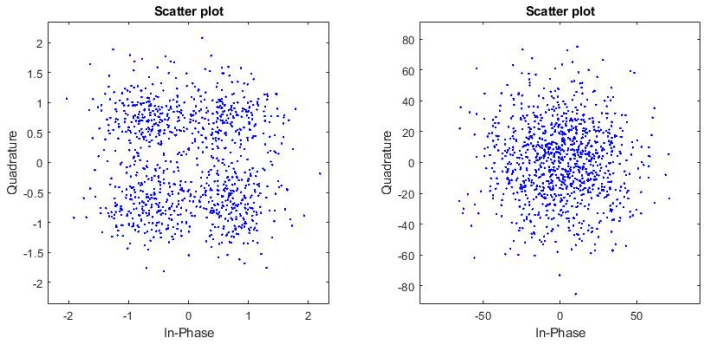

(a) 3rd channel reception (b) 4th channel reception

Figure 5.25: Channel 3 and 4 reception with an antenna's angular spacing of 1°

In Figure 5.25b we already see clearly how we have completely lost channel 4, as we can not recover a large percentage of transmitted symbols. While at the same time, channel 3 (Figure 5.25a) is is in a situation similar to channel 4 in the previous case. We can recover a lot of the transmitted symbols, but due to noise, we cannot guarantee 100% efficiency, causing us to consider the loss of channel 3 and guaranteeing the fully utility of the first two channels.

In the code we can make a command when calculating the H matrix, that when surpassing a level of 7dB of SNR, that channel is cancelled, so the power allocated to that channel is distributed among the others.

The Signal power of this case is the following:

		Receiver			
		1	2	3	4
CHANNEL	1	65,9	48,7	22,7	16,5
	2	65,9	48,7	22,7	16,5
	3	65,9	48,7	22,7	16,5
	4	65,9	48,7	22,7	16,5

Table 5.21: Signal power for each receiver with an angular spacing of 1°

In this case we check that both receiver 3rd the signal power starts to be enough similar to that of noise (16.5dBW), so there will be symbols that we will not be able to receive. While the power with the 4th receiver is equal to the noise, therefore the received symbols will be seen too affected to recover.

5.4.1 Measurements of the limit angles

To end this project, the channel lost test will be carried out in the anechoic chamber to proof that the results of the simulations also happens in the real scenario.

We will start with the case where only the 4th channel was lost, that is the one with the antenna's angular spacing of 4°. Firstly the H matrix 5.23 is estimated with the same code used previously (calMIMO), in order to realize all the MIMO transmission process.

H= 100*

-2.7121 - 1.0185i	-3.2780 + 0.9595i	2.3622 - 2.3513i	2.8302 - 0.8669i
-2.7281 + 0.7444i	-3.0276 + 1.6450i	2.7688 - 1.7539i	2.7281 + 0.9397i
-1.7056 + 2.0816i	-2.5594 + 2.1512i	2.9364 - 0.9782i	1.5543 + 2.3464i
-0.0616 + 2.5125i	-2.0341 + 2.6249i	2.9656 - 0.2862i	-0.2656 + 2.6754i

Table 5.22: H matrix 4Tx and 4 Rx in anechoic chamber with 4° angle spacing

With this measures done, we also confirmed that, the noise power, signal power and the symbol errors at the receiver were similar to the previous measurements done, so the comparison between results could be done.

The final step is to do the transmission in the anechoic chamber with the code (Execucio1) four times, representing the 4 receivers. When all the four transmissions are made, the final reception for all the four channels is seen in the following Figures 5.28 and 5.28:

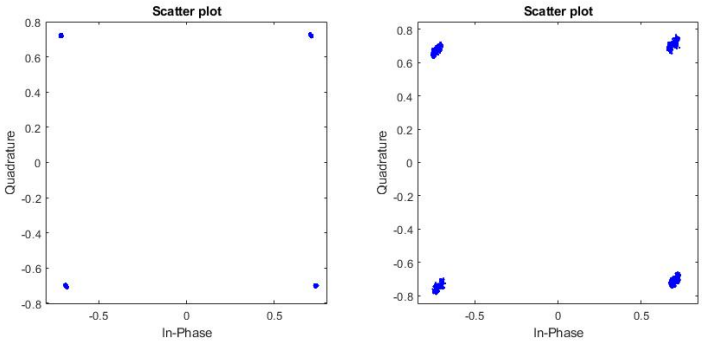

(a) 1st channel reception (b) 2nd channel reception

Figure 5.26: Measures of channel 1 and 2 reception with an antenna's angular spacing of 4°

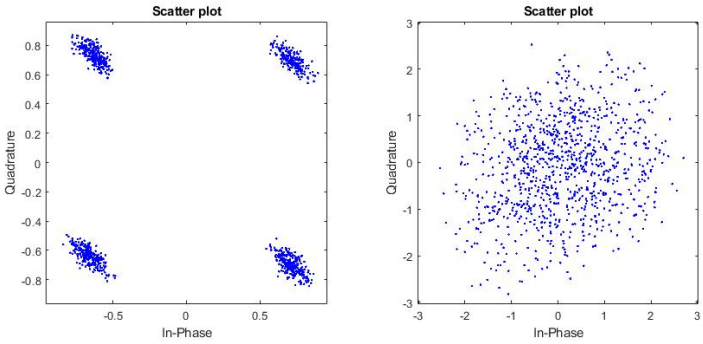

(a) 3rd channel reception (b) 4th channel reception

Figure 5.27: Measures of channel 3 and 4 reception with an antenna's angular spacing of 4°

In this measurement we confirm that the 4th channel starts fading and not all the transmitted symbols are able to be well received, just as the simulation.

If we look to the scenario were the antenna's angular spacing was 1°, the channel matrix 3.12 was the following:

H= 100*

-2.7112 - 1.0043i	-3.2704 + 0.9538i	2.3448 - 2.3323i	2.8287 - 0.8594i
-2.8118 - 0.5498i	-3.2482 + 1.1675i	2.4913 - 2.2560i	2.9262 - 0.4718i
-2.8650 - 0.1740i	-3.1622 + 1.2736i	2.5579 - 2.0470i	2.9387 + 0.0624i
-2.8371 + 0.3301i	-3.1105 + 1.5508i	2.6986 - 1.9462i	2.8695 + 0.4670i

Table 5.23: H matrix 4Tx and 4 Rx in anechoic chamber with 1° angle spacing

The final transmission confirms what we saw in the simulation, that the 3rd channel is not able to receive correctly all the symbols while the 4th channel has been completely interfered due to the noise.

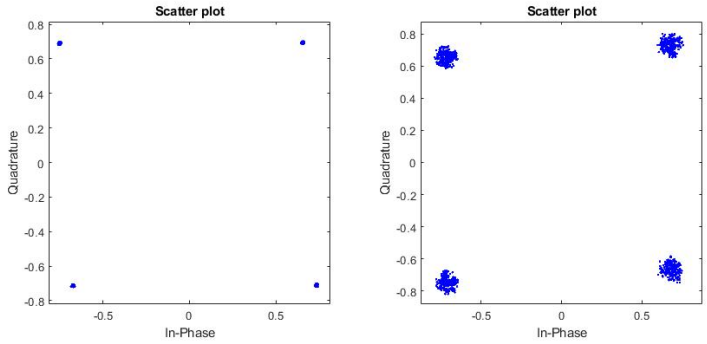

(a) 1st channel reception (b) 2nd channel reception

Figure 5.28: Measures of channel 1 and 2 reception with an antenna's angular spacing of 1°

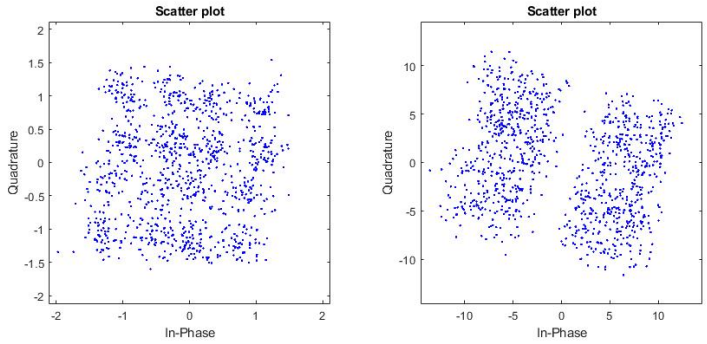

(a) 3rd channel reception (b) 4th channel reception

Figure 5.29: Measures of channel 3 and 4 reception with an antenna's angular spacing of 1°

Chapter 6

Conclusions and future work

6.1 Conclusions

In this thesis, the basic concepts of the design and fabrication of a patch antenna has been presented. We have simulated and measured some of the antenna's parameter to see that it can be used for the application it has been made for. This procedures try to promote and develop the study of the created designs in order for them to fulfill its requirements. As we have seen during Chapters 2 and 3, although patch antennas are not a newly technology and has been used for decades. It is very interesting to the uses it can be given for the new 5G applications, such as MIMO transmission. As in every project the technology, in this case the antenna, has to be fabricated in some conditions, such as dimensions and operating frequency. This conditions of 3.6GHz working frequency and 290x70mm of maximum surface have been accomplished both in simulations and real measurements of the array not without adjustments that have also been described in this thesis. This procedure have been analysed with the software FEKO, and the anechoic chamber of Universitat Autònoma de Barcelona.

The final objective of this thesis was to carry out a MIMO transmission with the SDR FMCOMMS5-EBZ evaluation board. To do so the concepts on which a MIMO transmission is based are explained in Chapter 4. MIMO transmission theory was discovered many years ago, but due to technology restrictions, mostly dimensions due to frequency, it could not have been implemented since this moment. Finally in Chapter 5 the study and development of the MIMO transmission was done both in simulations and in a real scenario thanks to the antenna previously fabricated. Both cases were done in our thesis increasing the channel capacity of the main channel. On the other hand, the limits of the transmission in our scenario, such as the minimum angle the antennas have to be in order to lose or gain channels and the powers of our system, has been tested and proved in the real transmission. This study promotes research into new technologies, that as many more, has the theoretical concepts developed but due to the technology restriction could not be implemented in a real life application.

6.2 Future work

The future work of this project is, exploring more of the MIMO transmission and its features, not only in the anechoic chamber but outside, to see a real scenario. To do so firstly, the different variation of our system could be explored, such as adding a reflection in the channel and how it could have been taken advantage of, since it can be seen as another array transmitting from that position. Instead of having 1 receiver and rotate the transmitter, add another array to the full real system as a receiver and see if this changes the different values of the channel.

Try to optimise the post-processing and if we see that some channel have an SNR that has been determined that will not allow the channel transmission, try to cancel that channel transmission so more power is distributed to the other channels.

The obvious progress in the project is trying to make this MIMO transmission outside the anechoic chamber to see how the channel changes and if with a real noise scenario the transmission can be done. Finally to make the application more complete, see how a scenario with a time-variant H matrix when objects and the distribution changes the calculus of this matrix is done. Because until now, this H measurement was done just 1 time and then all the transmissions had the same channel matrix. But if it changes, the transmission must take this into account to work well.

Another working aspect of the project would be try to apply this MIMO transmission technology in a real life application. Could be done in a static channel since the antennas may not be portable or if it is possible to decrease the antenna dimensions add them into a portable device.

Appendix A

Appendix

A.1 asysol2feko$_ffe$

Code that will be used to adapt the anechoic chamber measurement to a .txt file that FEKO can read. Useful to compared the results.

```
function asysol2feko_ffe(name_f,freq)

%% Conversion of asysol txt file to ffe file than can be read with feko
name_f= '20212610_Patch4_array_5_pEpH_FR_003600.TXT';
freq=3.6e9;

f_in=fopen(name_f,'r');

%Load header input file
tline = fgets(f_in);%Date
tline = fgets(f_in);%Operator

tline = fgets(f_in);%Description
f_format='';
if ~isempty(findstr(tline,'Real and Imaginary')); f_format='re_im';end;
if ~isempty(findstr(tline,'Magnitude dB and Phase deg')); f_format='mg_ph';end;

tline = fgets(f_in);%Aux. axis we suppose both th and ph components always

tline = fgets(f_in);%Step axis (azimuth)
aux_line=tline(10:end); c_pos=find(aux_line==',');aux_line(c_pos)='.';
azimuth_aux=str2num(aux_line);
theta=azimuth_aux(1):azimuth_aux(3):(azimuth_aux(2)+azimuth_aux(3));
```

```
n_theta=length(theta);

tline = fgets(f_in);%Scan axis (roll)
aux_line=tline(10:end);c_pos=find(aux_line==',');aux_line(c_pos)='.';
roll_aux=str2num(aux_line);
phi=roll_aux(1):roll_aux(3):(roll_aux(2)+roll_aux(3));
n_phi=length(phi);

% [phph,thth]=meshgrid(phi,theta);
% kx=sind(thth).*cosd(phph);ky=sind(thth).*sind(phph);kz=cosd(thth);
% thth_b=acos(kz)*180/pi;
% theta=unique(round(thth_b))';theta=[theta theta(end)+azimuth_aux(3)];
% n_theta=length(theta);
% phph_b=mod(atan2(ky,kx)*180/pi,360);
% phi=unique(round(phph_b))';phi=[phi phi(end)+roll_aux(3)];
% n_phi=length(phi);

Eth=zeros(n_theta,n_phi);Dth=zeros(n_theta,n_phi);%Initialize matrix
Eph=zeros(n_theta,n_phi);Dph=zeros(n_theta,n_phi);%Initialize matrix
Dtot=zeros(n_theta,n_phi);

tline = fgets(f_in);%empty line
tline = fgets(f_in);%empty line
tline = fgets(f_in);%empty line
tline = fgets(f_in);%empty line
tline = fgets(f_in);%empty line
tline = fgets(f_in);%column header

 while 1
        tline = fgets(f_in);
        if ~ischar(tline),
            break;
        end
        c_pos=find(tline==',');tline(c_pos)='.';
        values=str2num(tline);
        aux_axis=values(1);
        step_axis=values(2);
        scan_axis=values(3);
        switch f_format
            case 're_im',
                Efield=values(4)+j*values(5);
            case 'mg_ph'
                Efield=(10^(values(4)/20))*exp(j*values(5)*pi/180);
```

```
            otherwise
                error('Formato de los datos no contemplado')
        end
%         kx=sind(step_axis).*cosd(scan_axis);ky=sind(step_axis).*sind(scan_axis);kz=
%         step_axis=round(acos(kz)*180/pi);
%         if sind(step_axis)==0,
%             scan_axis=round(mod(atan2(sind(scan_axis),cosd(scan_axis))*180/pi,360))
%         else
%             scan_axis=round(mod(atan2(ky,kx)*180/pi,360));
%         end;


        pos_th=find(abs(theta-step_axis)<1e-6);
        pos_ph=find(abs(phi-scan_axis)<1e-6);

        if step_axis >= 180, Efield=-Efield;end
        switch aux_axis %Ojo, los case pueden ser diferente seg n como se coloque la
            case 0
                Eth(pos_th,pos_ph)=Efield;
                Dth(pos_th,pos_ph)=Efield*conj(Efield);
            case 90
                Eph(pos_th,pos_ph)=Efield;
                Dph(pos_th,pos_ph)=Efield*conj(Efield);
            otherwise
                error('lectura linea incorrecta');
        end;
 end;

Eth(:,end)=(Eth(:,1));%Add extra column to close sphere
Eph(:,end)=(Eph(:,1));%Add extra column to close sphere
Dth(:,end)=(Dth(:,1));%Add extra column to close sphere
Dph(:,end)=(Dph(:,1));%Add extra column to close sphere

fclose(f_in);

%Directivity
Dtot=Dth+Dph;
ttot=Dtot/max(max(Dtot));
tth=Dth/max(max(Dtot));
tph=Dph/max(max(Dtot));

Dmax=10*log10(4*pi/(sum(sum(ttot.*abs(sind(theta'*ones(size(phi))))))*azimuth_aux(3)*
Dtot=10*log10(ttot)+Dmax;
```

```
Dth=10*log10(tth)+Dmax;
Dph=10*log10(tph)+Dmax;

%write file

f_out=fopen(strcat(name_f(1:end-4),'.ffe'),'w');

tline='##File Type: Far field\n';fprintf(f_out,tline);
tline='##File Format: 3\n';fprintf(f_out,tline);
tline='##Source: converted from asysol\n';fprintf(f_out,tline);
tline='##Date: 2016-07-02 16:59:19\n';fprintf(f_out,tline);
tline='** File exported by FEKO kernel version 7.0-391\n';fprintf(f_out,tline);
tline='\n';fprintf(f_out,tline);
tline='#Request Name: FarField1 \n';fprintf(f_out,tline);
tline=sprintf('#Frequency: %e\n',freq);fprintf(f_out,tline);
tline='#Coordinate System: Spherical\n';fprintf(f_out,tline);
tline=sprintf('#No. of Theta Samples: %d\n',n_theta);fprintf(f_out,tline);
tline=sprintf('#No. of Phi Samples: %d\n',n_phi);fprintf(f_out,tline);
tline='#Result Type: Directivity\n';fprintf(f_out,tline);
tline='#No. of Header Lines: 1\n';fprintf(f_out,tline);
tline='#       "Theta"              "Phi"            "Re(Etheta)"
"Im(Etheta)"        "Re(Ephi)"          "Im(Ephi)"    "Directivity(Theta)" "Directivity(Phi)"
fprintf(f_out,tline);

[phph,thth]=meshgrid(phi,theta);thth=thth(:);phph=phph(:);

var=[thth phph real(Eth(:)) imag(Eth(:)) real(Eph(:)) imag(Eph(:)) Dth(:) Dph(:) Dtot(:)];

for cont=1:(n_theta*n_phi),
    tline=num2str(var(cont,:));
    fprintf(f_out,strcat(tline,'\n'));
end;

tline='\n';fprintf(f_out,tline);

fclose(f_out);

return
%!type MovilAntenna_900_3_JP_000800.ffe MovilAntenna_900_000840.ffe
MovilAntenna_1500_000880.ffe MovilAntenna_1800_000920.ffe MovilAntenna_2100_000960.ffe> ou

%!type 20190409_stackpatch_p1_00*.ffe > out.ffeMovilAntenna_1500_000880.ffe MovilAntenna_1
```

A.2 H matrix simulation

In this section there will be the code used to extract the H matrix from a certain number of receiving/-transmitting antennas:

```
clear all
format short

a=1
n_t=4;%nummero de antenas transmisoras
d_t=1;%distancia entre antenas transmisoras (norm. lambda)
phi_t=0;%rotacion del antenas transmisoras respecto eje z (eje x, phi=0)
phi=90; %angle d'incid ncia
phi1=1.82;
lam=3e8/3.6e9;
d=2.6/lam; %Distancia entre arrays (norm. lambda)
n_r=1; %numero arrays
n_rat=1; %numero antenes per array (EN AQUEST CAS NOMESS TENIM 1 ANTENA)
d_mat=zeros(n_r,n_t);
H=zeros(n_r,n_t);

%CALCUL DE LA DISTANCIA ENTRE ANTENES TX I LA PRIMERA ANETNA DE REFERENCIA
%DEL ARRAY ()
for k1=1:n_rat
for k2=1:n_t
d_mat(k1,k2)= (d+(abs(k2-k1)*phi1)/(sqrt((abs(k2-k1))^2)+d^2))*lam;
end
end

%OBTENIM LA MATRIU QUE ENS DESCRIU LA DIFERENCIA EN
%DISTANCIES DE LES DIFERENTS ANTENES PAG 9 FORMULA 7.21
er=zeros(n_rat,n_t);
for k3=1:n_rat
for k4=1:n_t
theta(k4)= phi+(k4-1)*phi1;
er(k3,k4)= exp(-i*2*pi*(k3-1)*cosd(theta(k4)));
end
end

q=1/(sqrt(n_rat));
er_f=q*er;

%CALCULEM LA MATRIU H
for k6=1:n_rat
```

```
for k5=1:n_t
 H(k6,k5)= a*sqrt(n_rat)*exp(-i*2*pi*d_mat(k5)/lam)*er_f(k6,k5);
end
end
H;
H_ref=H;
[U,S,V]= svd(H);
S
H
```

A.3 QPSK transmission

```
n_simb=1024;% # symbols per frame
X=linspace(-sqrt(2)/2,sqrt(2)/2,sqrt(M));
simb_TX=XX+1i*YY;simb_TX=simb_TX(:).';% Available symbols
for cont=1:nframe
s_ini=simb_TX(randi(M,1,n_simb-2));%random symbols to transmit
simb=repmat([0 0 s_ini],l_s,1);
simb=simb(:);%Enlarge pulses to avoid distortion
ch_1i_data(:,1,cont)=real(simb*1);
ch_1q_data(:,1,cont)=imag(simb*1);
s_ini=simb_TX(randi(M,1,n_simb-2));%random symbols to transmit
simb=repmat([0 0 s_ini],l_s,1);
simb=simb(:);%Enlarge pulses to avoid distortion
ch_2i_data(:,1,cont)=real(simb*1);
ch_2q_data(:,1,cont)=imag(simb*1);
s_ini=simb_TX(randi(M,1,n_simb-2));%random symbols to transmit
simb=repmat([0 0 s_ini],l_s,1);
simb=simb(:);%Enlarge pulses to avoid distortion
ch_3i_data(:,1,cont)=real(simb*1);
ch_3q_data(:,1,cont)=imag(simb*1);
s_ini=simb_TX(randi(M,1,n_simb-2));%random symbols to transmit
simb=repmat([0 0 s_ini],l_s,1);
simb=simb(:);%Enlarge pulses to avoid distortion
ch_4i_data(:,1,cont)=real(simb*1);
ch_4q_data(:,1,cont)=imag(simb*1);
end
Xf= [ch_1i_data+i*ch_1q_data ch_2i_data+i*ch_1q_data ch_3i_data+i*ch_1q_data ch_4i_da
```

A.4 calMIMO

Obtaining the channel matrix in the anechoic chamber. This code must be tranmsitted n_r times in order to simulate the number of receive antennas at their respective position.

```
%% Parte para calibrar

fs=30.72e6;Ts=1/fs;%Sampling frequency
n_simb=1024;% # symbols per frame
l_s=10; % # samples in a symbol
nframe=15;% # frames

M=4; %QPSK = 4, 16-QAM = 16
X=linspace(-sqrt(2)/2,sqrt(2)/2,sqrt(M));
Y=X;
[YY,XX]=meshgrid(Y,X);
simb_TX=XX+1i*YY;simb_TX=simb_TX(:).';% Available symbols

lframe=n_simb*l_s;% length frame in samples
t_series=[0:(nframe-1)]*lframe*Ts;%time frames
inputchannel=lframe;
outputchannel=lframe;
stop_time=nframe*lframe*Ts;%Simulink simulation time

%Initialize channels
ch_1i_data=zeros(lframe,1,nframe);
ch_1q_data=zeros(lframe,1,nframe);
ch_2i_data=zeros(lframe,1,nframe);
ch_2q_data=zeros(lframe,1,nframe);
ch_3i_data=zeros(lframe,1,nframe);
ch_3q_data=zeros(lframe,1,nframe);
ch_4i_data=zeros(lframe,1,nframe);
ch_4q_data=zeros(lframe,1,nframe);

s_ini=zeros(nframe,n_simb-2);%Initialize record of transmitted symbols

%% Simulacion de los canales

%%%% Channel 1

%%inicializaci n secuencia a enviar

    s_ini=simb_TX(randi(M,1,n_simb-2));%random symbols to transmit
```

```
    simb=repmat([0 0 s_ini],l_s,1);simb=simb(:);%Enlarge pulses to avoid distortion

for cont=1:nframe

    ch_1i_data(:,1,cont)=real(simb*1);
    ch_1q_data(:,1,cont)=imag(simb*1);

    ch_2i_data(:,1,cont)=real(simb*0);
    ch_2q_data(:,1,cont)=imag(simb*0);

    ch_3i_data(:,1,cont)=real(simb*0);
    ch_3q_data(:,1,cont)=imag(simb*0);

    ch_4i_data(:,1,cont)=real(simb*0);
    ch_4q_data(:,1,cont)=imag(simb*0);

end
%Utilitzarem unicament una secuencia perque ens encaixin els resultats i
%sigui la mateixa a tot arreu. Per aixo als altres esta comentat

%Build time series that feed the simulink model
ch_1i=timeseries(ch_1i_data,t_series);
ch_1q=timeseries(ch_1q_data,t_series);

ch_2i=timeseries(ch_2i_data,t_series);
ch_2q=timeseries(ch_2q_data,t_series);

ch_3i=timeseries(ch_3i_data,t_series);
ch_3q=timeseries(ch_3q_data,t_series);

ch_4i=timeseries(ch_4i_data,t_series);
ch_4q=timeseries(ch_4q_data,t_series);

sim('qpsk_4ch.slx',stop_time)
ch_cali=timeseries(ch_1i_data,t_series);
ch_calq=timeseries(ch_1q_data,t_series);

%load RX1_1.mat

cal_cconv_frame
ch1_corr=S_corr;

%%%% Channel 2
```

```
for cont=1:nframe
%     s_ini(cont,:)=simb_TX(randi(M,1,n_simb-2));%random symbols to transmit
%     simb=repmat([0 0 s_ini(cont,:)],l_s,1);simb=simb(:);%Enlarge pulses to avoid distorti

    ch_1i_data(:,1,cont)=real(simb*0);
    ch_1q_data(:,1,cont)=imag(simb*0);

    ch_2i_data(:,1,cont)=real(simb*1);
    ch_2q_data(:,1,cont)=imag(simb*1);

    ch_3i_data(:,1,cont)=real(simb*0);
    ch_3q_data(:,1,cont)=imag(simb*0);

    ch_4i_data(:,1,cont)=real(simb*0);
    ch_4q_data(:,1,cont)=imag(simb*0);

end

%Build time series that feed the simulink model
ch_1i=timeseries(ch_1i_data,t_series);
ch_1q=timeseries(ch_1q_data,t_series);

ch_2i=timeseries(ch_2i_data,t_series);
ch_2q=timeseries(ch_2q_data,t_series);

ch_3i=timeseries(ch_3i_data,t_series);
ch_3q=timeseries(ch_3q_data,t_series);

ch_4i=timeseries(ch_4i_data,t_series);
ch_4q=timeseries(ch_4q_data,t_series);

sim('qpsk_4ch.slx',stop_time)
ch_cali=timeseries(ch_2i_data,t_series);
ch_calq=timeseries(ch_2q_data,t_series);

%load RX1_2.mat
cal_cconv_frame
ch2_corr=S_corr;

%%%% Channel 3

for cont=1:nframe
```

```
%      s_ini(cont,:)=simb_TX(randi(M,1,n_simb-2));%random symbols to transmit
%      simb=repmat([0 0 s_ini(cont,:)],l_s,1);simb=simb(:);%Enlarge pulses to avoid di

    ch_1i_data(:,1,cont)=real(simb*0);
    ch_1q_data(:,1,cont)=imag(simb*0);

    ch_2i_data(:,1,cont)=real(simb*0);
    ch_2q_data(:,1,cont)=imag(simb*0);

    ch_3i_data(:,1,cont)=real(simb*1);
    ch_3q_data(:,1,cont)=imag(simb*1);

    ch_4i_data(:,1,cont)=real(simb*0);
    ch_4q_data(:,1,cont)=imag(simb*0);

end

%Build time series that feed the simulink model
ch_1i=timeseries(ch_1i_data,t_series);
ch_1q=timeseries(ch_1q_data,t_series);

ch_2i=timeseries(ch_2i_data,t_series);
ch_2q=timeseries(ch_2q_data,t_series);

ch_3i=timeseries(ch_3i_data,t_series);
ch_3q=timeseries(ch_3q_data,t_series);

ch_4i=timeseries(ch_4i_data,t_series);
ch_4q=timeseries(ch_4q_data,t_series);

sim('qpsk_4ch.slx',stop_time)
ch_cali=timeseries(ch_3i_data,t_series);
ch_calq=timeseries(ch_3q_data,t_series);

%load RX1_3.mat

cal_cconv_frame
ch3_corr=S_corr;

%%%% Channel 4

for cont=1:nframe
%      s_ini(cont,:)=simb_TX(randi(M,1,n_simb-2));%random symbols to transmit
```

```
%      simb=repmat([0 0 s_ini(cont,:)],l_s,1);simb=simb(:);%Enlarge pulses to avoid distorti

    ch_1i_data(:,1,cont)=real(simb*0);
    ch_1q_data(:,1,cont)=imag(simb*0);

    ch_2i_data(:,1,cont)=real(simb*0);
    ch_2q_data(:,1,cont)=imag(simb*0);

    ch_3i_data(:,1,cont)=real(simb*0);
    ch_3q_data(:,1,cont)=imag(simb*0);

    ch_4i_data(:,1,cont)=real(simb*1);
    ch_4q_data(:,1,cont)=imag(simb*1);

end

%Build time series that feed the simulink model
ch_1i=timeseries(ch_1i_data,t_series);
ch_1q=timeseries(ch_1q_data,t_series);

ch_2i=timeseries(ch_2i_data,t_series);
ch_2q=timeseries(ch_2q_data,t_series);

ch_3i=timeseries(ch_3i_data,t_series);
ch_3q=timeseries(ch_3q_data,t_series);

ch_4i=timeseries(ch_4i_data,t_series);
ch_4q=timeseries(ch_4q_data,t_series);

sim('qpsk_4ch.slx',stop_time)
ch_cali=timeseries(ch_4i_data,t_series);
ch_calq=timeseries(ch_4q_data,t_series);

%load RX1_4.mat
cal_cconv_frame
ch4_corr=S_corr;

H_30_10=[ch1_corr ch2_corr ch3_corr ch4_corr]

save H_30_10.mat H_30_10 ;
```

A.5 calconvframe

Alignement of the 4 streams transmitted streams in order to compare them properly

```
%nframe=10;
%lframe=768;
%l_s=128;
contframe=10;
refconv=zeros(lframe,1);refconv(1:(2*l_s))=1;

simbinicial=zeros((lframe-2*l_s)/l_s,contframe);
simbfinal=zeros((lframe-2*l_s)/l_s,contframe);
for cont=1:contframe,
    %cont
    yyy=RX1.data(:,1,cont+4);yyy=yyy(:);
    ref=ch_cali.data((2*l_s+1):end,1,cont+1)+j*ch_calq.data((2*l_s+1):end,1,cont+1);r

    xxx=cconv(abs(yyy),refconv,lframe);
    %plot(abs(xxx));

    pos_min=find(xxx==min(xxx));pos_min=mod(pos_min+1-2*l_s,lframe);

    zzz=circshift(yyy,-pos_min);
    vvv=zzz((2*l_s+1):end);

    simbinicial(:,cont)=ref((l_s/2):l_s:end);
    simbfinal(:,cont)  =vvv((l_s/2):l_s:end);
end;

S_corr=conj(mean(simbfinal(:)./simbinicial(:)))
S_L=mean(abs(simbfinal(:)))

save inicial_30_4 simbinicial
save final_30_4 simbfinal
save corr_30_4 S_corr
```

A.6 Executioncode

MIMO transmission that will implement the pre/post processing with the channel matrix. This process will also be transmitted n_r times

```
%% Parte para calibrar

fs=30.72e6;Ts=1/fs;%Sampling frequency
n_simb=1024;% # symbols per frame
l_s=10; % # samples in a symbol
nframe=15;% # frames

M=4; %QPSK = 4, 16-QAM = 16
X=linspace(-sqrt(2)/2,sqrt(2)/2,sqrt(M));
Y=X;
[YY,XX]=meshgrid(Y,X);
simb_TX=XX+1i*YY;simb_TX=simb_TX(:).';% Available symbols

lframe=n_simb*l_s;% length frame in samples
t_series=[0:(nframe-1)]*lframe*Ts;%time frames
inputchannel=lframe;
outputchannel=lframe;
stop_time=nframe*lframe*Ts;%Simulink simulation time

%Initialize channels
ch_1i_data=zeros(lframe,1,nframe);
ch_1q_data=zeros(lframe,1,nframe);
ch_2i_data=zeros(lframe,1,nframe);
ch_2q_data=zeros(lframe,1,nframe);
ch_3i_data=zeros(lframe,1,nframe);
ch_3q_data=zeros(lframe,1,nframe);
ch_4i_data=zeros(lframe,1,nframe);
ch_4q_data=zeros(lframe,1,nframe);

s_ini1=repmat([0 0 simb_TX(randi(M,1,n_simb-2))], l_s , 1); s_ini1=s_ini1(:);
s_ini2=repmat([0 0 simb_TX(randi(M,1,n_simb-2))], l_s , 1); s_ini2=s_ini2(:);
s_ini3=repmat([0 0 simb_TX(randi(M,1,n_simb-2))], l_s , 1); s_ini3=s_ini3(:);
s_ini4=zeros(size(s_ini3)); %Canal que son 0 porque no usaremos

simb=[s_ini1.' ; s_ini2.' ; s_ini3.' ; s_ini4.' ];

load('H_0_10.mat');
load('H_10_10.mat');
```

```
load('H_20_10.mat');
load('H_30_10.mat');

H=[H_0_10;H_10_10;H_20_10;H_30_10]
H

[U,S,V] = svd(conj(H));
S
U
V
cod = V*simb;

%% Part a repetir per a cada execuci

for cont=1:nframe

    ch_1i_data(:,1,cont)=real(cod(1,:));
    ch_1q_data(:,1,cont)=imag(cod(1,:));

    ch_2i_data(:,1,cont)=real(cod(2,:));
    ch_2q_data(:,1,cont)=imag(cod(2,:));

    ch_3i_data(:,1,cont)=real(cod(3,:));
    ch_3q_data(:,1,cont)=imag(cod(3,:));

    ch_4i_data(:,1,cont)=real(cod(4,:));
    ch_4q_data(:,1,cont)=imag(cod(4,:));

end

%Build time series that feed the simulink model
ch_1i=timeseries(ch_1i_data,t_series);
ch_1q=timeseries(ch_1q_data,t_series);

ch_2i=timeseries(ch_2i_data,t_series);
ch_2q=timeseries(ch_2q_data,t_series);

ch_3i=timeseries(ch_3i_data,t_series);
ch_3q=timeseries(ch_3q_data,t_series);

ch_4i=timeseries(ch_4i_data,t_series);
ch_4q=timeseries(ch_4q_data,t_series);
```

```
sim('qpsk_4ch.slx',stop_time)


simbfinal=zeros((lframe-2*l_s)/l_s,contframe);
for cont=1:contframe

    yyy=RX1.data(:,1,cont+4);yyy=yyy(:);
    ref=ch_4i.data((2*l_s+1):end,1,cont+1)+j*ch_4q.data((2*l_s+1):end,1,cont+1);ref=ref(:)

    xxx=cconv(abs(yyy),refconv,lframe);

    pos_min=find(xxx==min(xxx));pos_min=mod(pos_min+1-2*l_s,lframe);

    zzz=circshift(yyy,-pos_min);
    vvv=zzz((2*l_s+1):end);

    simbfinal(:,cont)  =vvv((l_s/2):l_s:end);
end

S_L=mean(abs(simbfinal(:)))

Out = mean(simbfinal,2);  % Fer la mitjana dels resultats
Out_15 = Out;

scatterplot(Out);

save Out_15.mat Out_15 ;

return

%% Resultat
Dec = [Out_0_5.' ; Out_5.' ; Out_10_5.';Out_15.'];
Resultat = pinv(S)*U'*Dec;
scatterplot(Resultat(:));
%%
for k=1:4
simbprova(k,:)=simb(k,(ls/2:l_s:end));
end

Comprovacio=Resultat-simbprova;

%scatterplot(Comprovacio(1,:));
%scatterplot(Comprovacio(2,:));
```

```
%scatterplot(Comprovacio(3,:));
%scatterplot(Comprovacio(4,:));
mitja3=var(Comprovacio(3,:));

scatterplot(Resultat(1,:))
scatterplot(Resultat(2,:))
scatterplot(Resultat(3,:))
scatterplot(Resultat(4,:))
```

A.7 noise

Noise of the channel that will be helpful in order to know the errors of the system and knowing if the channel has changed. If it has changed the SNR means that the scenarios are not the same and can not be compared.

```
%prova de soroll%%
%En el notre cas tenim QPSK (4 simbols) per canal i 16 canals (4 RX 4
TX)
load('corr_0_4'); %s'incorpora la mostra de la correcci  aplicada a la mesura
load('final_0_4'); %s'incorpora la senyal rebuda per aquell angle i per aquell canal
load('inicial_0_4'); %s'incorpora la senyal transmesa per aquell angle i per aquell canal
inicial= simbinicial(:);
final= simbfinal(:);
l=length(final);
STX=unique(inicial)
%scatterplot(inicial) %veiem el que hem transm s
scatterplot(final) %veiem el que hem
simbol1=find(inicial==STX(1)); %busquem quants simbols dels 4 hem
transm s
simbol2=find(inicial==STX(2));
simbol3=find(inicial==STX(3));
simbol4=find(inicial==STX(4));
A=length(simbol1);
B=length(simbol2);
C=length(simbol3);
D=length(simbol4);
scatterplot(inicial(simbol1));
scatterplot(final(:)); %compte que no se si estan organitzats iguals
SRX=[mean(final(simbol1));mean(final(simbol2));mean(final(simbol3));me
an(final(simbol4))]; %fem la mitja de cada s mbol rebut per saber on
cau exactament la correcci
corr=conj(SRX./STX); % Fem el conjugat de la relaci  entre TX i RX
per tal de saber la correcci  que hauria de tenir cada s mbol
correccio= mean(corr); %veiem com hi ha un petit canvi en la correcci
aplicada tot i que es m nim,aquest canvi es
 %degut a que aqui es fa una mitja per cada
s mbol de la mesura final, mentre que
plot(SRX/correccio','x') %aqui ja s'ha aplicat la correccio be
hold on
plot(STX,'o')
%ARA MIREM LA PART DE LA POTENCIA
P=(final'*final)/l; %VALOR AL QUADRAT DE CADA PUNT DE LA TRANSMISSIO
PER LA QUANTITAT DE VALORS TRANSMESSOS (POTENCIA)
```

```
PLOG=10*log10(P);%HO PASSEM A LOGARITM

%SIMBOLS
%SIMBOL1
P1=final(simbol1)'*final(simbol1)/A;
P1L= 10*log10(P1);
S1REF=mean(final(simbol1));
N1=final(simbol1)-S1REF;
NOISE1=10*log10(std(N1))
%SIMBOL2
P2=final(simbol2)'*final(simbol2)/B;
P2L= 10*log10(P2);
S2REF=mean(final(simbol2));
N2=final(simbol2)-S2REF;
NOISE2=10*log10(std(N2))
%SIMBOL3
P3=final(simbol3)'*final(simbol3)/C;
P3L= 10*log10(P3);
S3REF=mean(final(simbol3));
N3=final(simbol3)-S3REF;
NOISE3=10*log10(std(N3));
%SIMBOL4
P4=final(simbol4)'*final(simbol4)/D;
P4L= 10*log10(P4);
S4REF=mean(final(simbol4));
N4=final(simbol4)-S4REF;
NOISE4=10*log10(std(N4));
%%FINAL
SFIN=[SRX(1)/correccio' SRX(2)/correccio' SRX(3)/correccio'
SRX(4)/correccio']
plot([SRX(1)/correccio' SRX(2)/correccio' SRX(3)/correccio'
SRX(4)/correccio'],'rd')
%RELACI DELS ERRORS
figure
plot([STX(1)*exp(j*pi) STX(2)*exp(j*pi/2) STX(3) STX(4)*exp(-
j*pi/2)],'bx')
hold on
plot([SRX(1)/correccio'*exp(j*pi) SRX(2)/correccio'*exp(j*pi/2)
SRX(3)/correccio' SRX(4)/correccio'*exp(-j*pi/2)],'rd')
ERROR= SRX/correccio'-STX;
scatterplot([N1; N2; N3; N4])
```

Bibliography

[1] E. Webster. Mimo (multiple input, multiple output). [Online]. Available: https://searchmobilecomputing.techtarget.com/definition/MIMO

[2] D. Tse and P. Viswanath, *Fundamentals of Wireless Communication*. Cambridge University Press, 2005.

[3] A. Devices. [Online]. Available: https://www.analog.com/en/products/ad9361.html

[4] M. de asuntos económicos y tranformación digital. Spain national table of frequency allocations. [Online]. Available: https://avancedigital.mineco.gob.es/espectro/Paginas/cnaf.aspx

[5] M. A. Khan and R. Vesilo, "A tutorial on siso and mimo channel capacities," 2021.

[6] gsma. (2019) Espectro 5g posición de política pública de la gsma.

[7] J. Salz, "Digital transmission over cross-coupled linear channels," *AT&T Technical Journal*, vol. 64, pp. 1147–1159, 1985.

[8] A. J. Paulraj., "Increasing capacty in wireless broadcast systems using distributed transmission/directional reception (dtdr)," 3 1992, uS Patent USOO5345599A. [Online]. Available: https://patents.google.com/patent/US5345599A/en

[9] E. B. Spangler, "Method and system for measurement of road profile," May 3 1988, uS Patent 4,741,207. [Online]. Available: http://www.google.it/patents/US4741207

[10] Metaswitch. What is 5g beamforming, beam steering and beam switching with massive mimo. [Online]. Available: https://www.metaswitch.com/knowledge-center/reference/what-is-beamforming-beam-steering-and-beam-switching-with-massive-mimo

[11] M. Ben Zid and K. Raoof, *Multi-User MIMO Communication : Basic Aspects, Benefits and Challenges*, 12 2013.

[12] J. Eilert, D. Wu, and D. Liu, "Efficient complex matrix inversion for mimo software defined radio," in *2007 IEEE International Symposium on Circuits and Systems (ISCAS)*, 2007, pp. 2610–2613.

[13] Altair. [Online]. Available: https://www.altair.com/feko/

[14] MATHWORKS. [Online]. Available: https://es.mathworks.com/products/matlab.html

[15] LPKF. [Online]. Available: http://www.lpkfusa.com/datasheets/prototyping/s62.pdf

[16] A. Devices. [Online]. Available: https://www.analog.com/en/design-center/evaluation-hardware-and-software/evaluation-boards-kits/eval-ad-fmcomms5-ebz.htmleb-overview

[17] keysight. [Online]. Available: https://www.keysight.com/es/en/assets/9018-04442/technical-specifications/9018-04442.pdf

[18] J. P. Granados, *Introduction to antennas*, 2021.

[19] ——, *Planar Antennas for Wireless Communications: Microstrip antennas*, 2021.

[20] everythingRF. [Online]. Available: https://www.antenna-theory.com/

[21] data alliance. [Online]. Available: https://www.data-alliance.net/blog/antenna-beamwidth/

[22] electronics desk. [Online]. Available: https://electronicsdesk.com/antenna-gain.html

[23] J. Howell, "Microstrip antennas," in *1972 Antennas and Propagation Society International Symposium*, vol. 10, 1972, pp. 177–180.

[24] Pasternack. [Online]. Available: https://www.pasternack.com/t-calculator-microstrip-ant.aspx

[25] WolframMathWorld. [Online]. Available: https://mathworld.wolfram.com/UnitaryMatrix.html

[26] R. Blahut, "Hypothesis testing and information theory," *IEEE Transactions on Information Theory*, vol. 20, no. 4, pp. 405–417, 1974.

[27]

[28] V. Meghdadi, "Ber calculation," *l Centro de Estudios de Telecomunicaciones (CETUC) de la Pontifica Universidad Católica de Rio de Janeiro*, 2008.